Short Length Scale Oxygen Isotope Heterogeneity in the Icelandic Mantle: Evidence from Plagioclase Compositional Zones

B. WINPENNY* AND J. MACLENNAN

DEPARTMENT OF EARTH SCIENCES, UNIVERSITY OF CAMBRIDGE, DOWNING STREET, CAMBRIDGE CB2 3EQ, UK

RECEIVED NOVEMBER 26, 2013; ACCEPTED NOVEMBER 11, 2014

Using a new high-resolution dataset, this study presents evidence for short length scale $^{18}O/^{16}O$ heterogeneity in the mantle source region of young (age ≤12 ka BP) Icelandic basalts. The dataset comprises secondary ion mass spectrometry determinations of $^{18}O/^{16}O$ in single compositional zones of plagioclase crystals from the primitive Borgarhraun flow in northern Iceland, along with trace and major element data from the same zones. The presence of mantle under Iceland with $\delta^{18}O$ below typical mid-ocean ridge basalt (MORB) values of ~5·5 ± 0·3‰ (VSMOW) has previously been disputed, because variability in $\delta^{18}O$ in many Icelandic basalts is also known to be caused by the interaction of basaltic melts with crustal lithologies that have been altered by low-$\delta^{18}O$ meteoric water. Primitive basalt flows, such as Borgarhraun, and their macrocrysts are the most likely candidates to retain a mantle $\delta^{18}O$ signature. However, the role of crustal processes in generating the low $\delta^{18}O$ in olivine crystals from these flows has not unequivocally been ruled out. By making intra-crystal analyses in Borgarhraun plagioclase it has been possible in this study to obtain a detailed record of the chemical and isotopic compositions of the melts that crystallized the plagioclase zones. The variability observed in trace element compositions of the early crystallized anorthitic plagioclase zones (80·9–89·4 mol % anorthite) is firstly shown to arise from melt compositional variability, and equilibrium melt concentrations of Sr, La and Y are then calculated from the crystal concentrations of these elements using carefully selected partition coefficients. The ranges of incompatible trace element ratios (La/Y, Sr/Y) in these equilibrium melts reflect a range of compositions of fractional mantle melts, a result that is in agreement with previous proposals for the cause of variability in trace element indices of Borgarhraun olivine-hosted melt inclusions and clinopyroxene compositional zones. Correlations observed between La/Y and Sr/Y in the melts in equilibrium with the Borgarhraun plagioclase zones and the $\delta^{18}O$ of these zones therefore support the hypothesis that the mantle under Iceland is heterogeneous in $^{18}O/^{16}O$. Such correlations have not previously been observed in intra-crystal data from Iceland, and provide strong evidence that mantle material with abnormally low $\delta^{18}O$ may exist in the form of readily fusible heterogeneities alongside ambient mantle with MORB-like $\delta^{18}O$ (≈+5·5‰) on a length scale of <100 km. The lowest $\delta^{18}O$ of plagioclase that is attributed to a mantle origin in this study is 4·5 ± 0·4‰, equating to a melt equivalent value of 4·3 ± 0·5‰ or an olivine equivalent value of 3·8 ± 0·5‰.

KEY WORDS: *Iceland; mid-ocean ridge; oxygen isotopes; plagioclase; trace elements*

INTRODUCTION

For around 40 years it has been known that many young (age ≤12 ka BP) Icelandic basalts have $^{18}O/^{16}O$ ratios that are outside the typical range for mid-ocean ridge basalts (MORB) (Muehlenbachs *et al.*, 1974). The range of MORB glasses, in $\delta^{18}O$ notation, is ~+5·2–5·8‰ VSMOW (Vienna Standard Mean Ocean Water) [Thirlwall *et al.* (2006) and references therein]; in comparison, the $\delta^{18}O$ values of fresh Icelandic basalts and basaltic glasses predominantly lie between ~+2 and ~+6‰ (e.g. Condomines *et al.*, 1983; Hémond *et al.*, 1988, 1993; Nicholson *et al.*, 1991; Sigmarsson *et al.*, 1991; Harmon & Hoefs, 1995; Burnard & Harrison, 2005; Macpherson *et al.*, 2005). Similarly large ranges are observed in crystals hosted in Icelandic basalts, and their melt inclusions (Gee *et al.*, 1998; Eiler *et al.*, 2000*a*, 2011; Skovgaard *et al.*, 2001; Breddam, 2002; Gurenko & Chaussidon, 2002; Maclennan

*Corresponding author. Telephone: +44 1223 333400. Fax: +44 1223 333450. E-mail: dbhw2@cam.ac.uk

et al., 2003*a*; Bindeman *et al.*, 2006, 2008; Thirlwall *et al.*, 2006). Studies of $\delta^{18}O$ in Icelandic basalts during the past 20 years have predominantly focused on analyses of fresh basaltic glass and large crystals hosted by basalts, typically by laser fluorination, as surficial processes may modify the oxygen isotope ratios of whole-rock samples (e.g. Burnard & Harrison, 2005).

Two origins for the production of low ($\lesssim$+5·5‰) and variable $\delta^{18}O$ in young Icelandic basalts have been proposed, which are not mutually exclusive. The first, widely accepted as causing $\delta^{18}O$ variability in many Icelandic basalts, is low-$\delta^{18}O$ Icelandic meteoric water, which creates hydrothermal fluids in the rift zones, which have similarly low values (−11 to −13‰ in northern Iceland; e.g. Kristmannsdóttir & Ármannsson, 2004). Assimilation of hydrothermally altered crustal lithologies by primary basaltic mantle melts with initial $\delta^{18}O$ of ~+5·5‰ will therefore result in a lowering of $\delta^{18}O$ in these melts. Hydrothermally altered crustal lithologies have a mean $\delta^{18}O$ of ~+2·0–4·5‰ (Gautason & Muehlenbachs, 1998), although values as low as −10·5‰ have been reported from geothermal boreholes (Hattori & Muehlenbachs, 1982).

The second origin, which has been a source of debate, is low-$\delta^{18}O$ material in the mantle melting region beneath Iceland (Muehlenbachs *et al.*, 1974). It has been postulated that $^{18}O/^{16}O$ variability exists in discrete heterogeneities under Iceland (e.g. Skovgaard *et al.*, 2001; Breddam, 2002; Gurenko & Chaussidon, 2002; Macpherson *et al.*, 2005) within a matrix of mantle with MORB-like $\delta^{18}O$ (≈+5·5‰; Mattey *et al.*, 1994). It has further been suggested that these isotopic heterogeneities may be hosted in lithological heterogeneities in the mantle (e.g. Maclennan *et al.*, 2003*a*; Stracke *et al.*, 2003*a*; Thirlwall *et al.*, 2006). Fractional mantle melting may sample such isotopic heterogeneities, and, depending on the extents and proportions in which the fractional melts mix prior to eruption, basalts with a range of $^{18}O/^{16}O$ ratios may be erupted. Globally, Iceland is not the only case where basalts may sample mantle heterogeneous in $\delta^{18}O$, as has been suggested from other studies on MORB (e.g. Eiler *et al.*, 2000*b*) and ocean island basalts. Ocean islands for which a mantle source of low $\delta^{18}O$ has been suggested include Hawaii (Eiler *et al.*, 1996), the Azores (Turner *et al.*, 2007) and the Canaries (Day *et al.*, 2009, 2010; Gurenko *et al.*, 2011). However, some researchers have not observed a mantle source for low $\delta^{18}O$ in basalts from these locations, notably Wang & Eiler (2008) and Garcia *et al.* (2013) for Hawaiian olivines and Genske *et al.* (2013) for olivines from the Azores.

A wealth of evidence has convincingly illustrated that assimilation of low-$\delta^{18}O$, hydrothermally altered Icelandic basalts, or partial melts thereof, can occur during fractional crystallization of basaltic melts in the crust (Condomines *et al.*, 1983; Macdonald *et al.*, 1987; Hémond *et al.*, 1988, 1993; Nicholson *et al.*, 1991; Sigmarsson *et al.*, 1991, 1992*a*, 1992*b*; Harmon & Hoefs, 1995; Gee *et al.*, 1998; Eiler *et al.*, 2000*a*; Burnard & Harrison, 2005; Bindeman *et al.*, 2006, 2008, 2012; Martin & Sigmarsson, 2007). The cause, however, of a low-$\delta^{18}O$ signature in some of the most primitive Icelandic basalts has been a source of debate [see, for instance, discussions by Eiler *et al.* (2000*a*), Maclennan *et al.* (2003*a*), Stracke *et al.* (2003a) and Bindeman *et al.* (2008)], as it is unlikely that such basalts have been affected by significant interaction with low-$\delta^{18}O$ crustal lithologies. Based on analyses of primitive basalts and their early crystallized products, some researchers have argued that the Icelandic mantle may contain low-$\delta^{18}O$ material. These studies and the ranges of $\delta^{18}O$ values that they ascribe to mantle O-isotope variability are summarized in Table 1. In the past few years, researchers working on the oxygen isotope compositions of basalts affected by crustal assimilation in Iceland have acknowledged that the Icelandic mantle may contain low-$\delta^{18}O$ material [Bindeman *et al.* (2008) suggested variability of <0·7‰], but the debate on the existence of low-$\delta^{18}O$ mantle under Iceland is not yet resolved. The continuing uncertainty hinges on the fact that studies that have attempted to determine mantle $^{18}O/^{16}O$ heterogeneity have performed $\delta^{18}O$ and other geochemical analyses on different length scales (whole-rock, crystal separate and intra-crystal analyses), and thus observed correlations between $\delta^{18}O$ and other indices have not unequivocally ruled out the role of crustal processes in generating low $\delta^{18}O$ in primitive Icelandic basalts. It is the aim of this contribution to present evidence from a detailed set of intra-crystal analyses that (1) low-$\delta^{18}O$ material exists as distinct heterogeneities in the mantle source region of Icelandic basalts, and (2) this low-$\delta^{18}O$ mantle material may exist in the form of readily fusible heterogeneities alongside refractory, depleted mantle with MORB-like $\delta^{18}O$ (≈+5·5‰).

O-isotope variability in primitive Theistareykir basalts

The Theistareykir volcanic system in northern Iceland is known for its primitive lava compositions that reflect some of the compositional variability of mantle melts (e.g. Elliott *et al.*, 1991; Hémond *et al.*, 1993; Slater *et al.*, 2001; Maclennan *et al.*, 2003*a*, 2003*b*; Stracke *et al.*, 2003*a*; Thirlwall *et al.*, 2004; Sims *et al.*, 2013). Melt inclusions in forsteritic olivines from Theistareykir lavas (Slater *et al.*, 2001) and from one well-studied flow in particular, Borgarhraun (Maclennan *et al.*, 2003*a*, 2003*b*), have also been shown to retain some of the compositional variability of mantle melts. Theistareykir samples, especially those from Borgarhraun, have therefore been regarded as a suitable place to look for the signature of mantle $\delta^{18}O$ variability (Eiler *et al.*, 2000*a*; Maclennan *et al.*, 2003*a*; Stracke

Table 1: Ranges in $\delta^{18}O$ ascribed to mantle $\delta^{18}O$ heterogeneity for Icelandic crystal phases and basaltic glasses

Olivine		Clinopyroxene		Plagioclase		Glass or WR		$\overline{\delta^{18}O_{melt}}$ of all phases			Reference
$\delta^{18}O_{melt}$	Fo	$\delta^{18}O_{melt}$	Mg#	$\delta^{18}O_{melt}$	An	$\delta^{18}O$	MgO	*n*	$\overline{\delta^{18}O}$	1σ	
						4·4–4·7	10·3–10·5	4	4·6	0·1	Breddam (2002)
2·9–7·4	86–90					4·0–6·2	8·6–11·4	55	5·6	0·8	Gurenko & Chaussidon (2002)
3·9–5·7	87–92	4·5–5·3	87–91				9·7–*19·0*	64	5·1	0·4	Maclennan et al. (2003b)
						4·6–4·6	9·6	3	4·6	0·0	Burnard & Harrison (2005)
4·5–5·6	n.d.					4·9–4·8	5·0–9·7	12	4·5	0·5	Macpherson et al. (2005)
5·0–5·9	n.d.						9·8–24·2	31	5·6	0·2	Kokfelt et al. (2006)
5·0–5·7	n.d.	5·2–5·6	n.d.	4·9–5·5	n.d.	5·3–5·8	*6·8–27·8*	65	5·2	0·3	Thirlwall et al. (2006)
4·7–5·7	75–88			4·8–5·4	71–91		*7·3–12·3*	11	5·0	0·3	Peate et al. (2009)
4·6–5·6	n.d.	5·1–5·6	n.d.	5·0–5·0	n.d.		*8·9–15·3*	20	5·1	0·3	Peate et al. (2010)

For the crystals or glass analysed for oxygen isotope ratios, ranges of olivine forsterite (Fo) contents, clinopyroxene Mg#, plagioclase anorthite (An) content and glass MgO content [or, in italics, the host basalt whole-rock (WR) MgO content, where no glass data exist] are given where these values were determined. It should be noted that many studies have not tied major or trace element compositions of crystals to $\delta^{18}O$ values of these crystals. Glass MgO values of Gurenko & Chaussidon (2002) include corrected melt inclusion data. $\delta^{18}O$ values of crystal phases are expressed as melt-equivalent values at 1260°C, using fractionations as follows: $\Delta^{18}O_{melt-olivine} = +0{\cdot}5‰$; $\Delta^{18}O_{melt-plagioclase} = -0{\cdot}2‰$; $\Delta^{18}O_{melt-clinopyroxene} = +0{\cdot}1‰$. The total number (*n*) of $\delta^{18}O$ analyses of phases, and the mean ($\overline{\delta^{18}O_{melt}}$) and standard deviations (σ) of their melt-equivalent values are also shown. The data of Skovgaard et al. (2001) are not listed as these were reinterpreted by Thirlwall *et al*. (2006).

et al., 2003*a*), as overprinting by crustal processes is less likely than in more evolved samples.

The origin of oxygen isotope variability in basalts from Theistareykir has been a topic of disagreement in past studies. Based on correlations of decreasing $\delta^{18}O$ in bulk crystal separates with whole-rock indices of enrichment (e.g. increasing K_2O/TiO_2 and La/Sm) and differentiation (e.g. Mg# and CaO/Na_2O), Eiler *et al.* (2000*a*) suggested that oxygen isotope ratios of some post-glacial Theistareykir basalts have been lowered by assimilation of melts of hydrothermally altered Icelandic crust, or mixing with crustally contaminated evolved basalts. On the other hand, Maclennan *et al.* (2003*a*), focusing on the primitive Borgarhraun flow, argued for a mantle origin of the $\delta^{18}O$ variability observed amongst single crystals from this flow. The method of Maclennan *et al.* (2003*a*) involved analysing olivine-hosted melt inclusions for trace elements by ion microprobe, and the host olivine crystal both for major elements by electron probe microanalysis (EPMA) and for oxygen isotope ratios by laser fluorination. The rationale behind the approach of Maclennan *et al.* (2003*a*) was that because crystals hosted by Icelandic basalts can be formed from single magma batches that mix prior to eruption (meaning that such crystals could be termed 'antecrysts'; Davidson *et al.*, 2007), earlier correlations observed between datasets obtained by sampling on different scales (e.g. major and trace element and radiogenic isotope analyses on whole-rock specimens, and O-isotope analyses in single crystals) have effectively spanned different statistical populations and are therefore ambiguous. However, Maclennan *et al.* (2003*a*) did not observe clear correlations between indices of enrichment in melt inclusions (e.g. La/Yb) and decreasing $\delta^{18}O$ of the host crystals. Eiler *et al.* (2011) performed seven ion microprobe analyses of $\delta^{18}O$ in Borgarhraun olivines but likewise did not see clear correlations. Such correlations might be expected if the low-$\delta^{18}O$ signature preserved in the Borgarhraun crystals originates in the mantle, and is associated with melts of fusible heterogeneities that are produced near the bottom of the melting region in the presence of garnet. The difficulty in establishing clear correlations was thought to be caused, at least in part, by the fact that the single, whole crystals analysed by laser fluorination could be zoned in $\delta^{18}O$.

Rationale for major element, trace element and isotopic analyses in plagioclase crystals

To overcome the problem of crystal $\delta^{18}O$ zoning, suspected by Maclennan *et al.* (2003*a*), and produce unequivocal correlations between geochemical indices, it is necessary to perform all analyses on an intra-crystal length scale. Because many incompatible trace elements that are useful in deciphering signals of mantle melting processes cannot be measured in olivine with good precision, this study has concentrated instead on major element, trace element and

oxygen isotope data gathered via microanalytical techniques from single compositional zones of anorthitic plagioclase crystals from the well-studied, primitive Borgarhraun flow. These plagioclase grains are shown below to have crystallized alongside the forsteritic Borgarhraun olivines analysed by Maclennan *et al.* (2003*a*). Because the analyses are all made within the same zones, observed correlations between elemental and isotopic datasets will be more robust than in previous studies. Recent work by Eiler *et al.* (2011) has indicated that variability of $<\sim 1‰$ can be clearly resolved in silicate minerals by secondary ion mass spectrometry (SIMS) techniques, with high accuracy and precision on single analyses [in the region of 0·2‰ and ±0·2‰ (1σ), respectively]. Therefore, obtaining a detailed record of $\delta^{18}O$ variation from Borgarhraun plagioclase compositional zones is potentially feasible.

Compositional zoning of Mg# and rare earth element (REE) concentrations is known to exist within early crystallized, high-Mg# clinopyroxene crystals from the Borgarhraun flow, which formed at ~1260°C (Maclennan *et al.*, 2003*a*; Winpenny & Maclennan, 2011). Diffusivities of REE at 1260°C (D^{1260}_{REE}) in clinopyroxene are $\sim 10^{-18}$ to $10^{-20}\,m^2\,s^{-1}$ (Sneeringer *et al.*, 1984; Van Orman *et al.*, 2001), and for Mg–Fe diffusion, $D^{1260}_{Mg-Fe} = 1{\cdot}4$–$8{\cdot}0 \times 10^{-18}\,m^2\,s^{-1}$ (Dimanov & Sautter, 2000; Dimanov & Wiedenbeck, 2006). For plagioclase, diffusivities of REE and Y at 1260°C are similar to those in clinopyroxene, at $\leq 2{\cdot}5 \times 10^{-18}\,m^2\,s^{-1}$ at 1260°C (Cherniak, 2002, 2010), and so the Borgarhraun plagioclase crystals that are crystallized concurrently with clinopyroxene should also preserve original compositional zoning in REE and Y. For Sr, the diffusion rate in anorthite at this temperature is slightly faster, at $4{\cdot}5 \times 10^{-18}$ to $2{\cdot}2 \times 10^{-17}\,m^2\,s^{-1}$ (Cherniak & Watson, 1992, 1994; Giletti & Casserly, 1994). Oxygen diffusivities (D_O) in plagioclase, although rapid under hydrothermal conditions, are affected to a negligible degree by the low water contents of primitive Icelandic basalts such as Borgarhraun (<0·5 wt % H_2O; Saal *et al.*, 2002; Nichols & Wysoczanski, 2007), increasing by $<0{\cdot}3 \log [D_O]$ units (Farver & Yund, 1990; Dixon *et al.*, 1995). Overall, oxygen diffusivities at 1260°C are very similar to the rate of Sr diffusion in plagioclase at this temperature, being $\sim 6 \times 10^{-18}\,m^2\,s^{-1}$ (Elphick *et al.*, 1988; Ryerson & McKeegan, 1994; Farver, 2010). Although storage for $\sim 10^3$–10^4 years at 1260°C could substantially reduce original Sr and $\delta^{18}O$ zoning in crystals of radius 1 mm, it is shown below that Borgarhraun plagioclase crystals retain zoning of Sr concentrations and $\delta^{18}O$. Nevertheless, the effect of Sr and O diffusion on the observations and correlations presented in this study will also be considered.

In this contribution it will be argued that variability in trace element ratios from high-anorthite Borgarhraun plagioclase compositional zones, co-crystallized in the lower Icelandic crust along with forsteritic olivine and high-Mg# clinopyroxene, reflect part of the range of chemical compositions produced by fractional melting of heterogeneous mantle. This is the same conclusion that was reached previously for olivine-hosted melt inclusions and clinopyroxene compositional zones from the same flow (Maclennan *et al.*, 2003*a*; Winpenny & Maclennan, 2011). Correlations between trace element ratios indicative of mantle melting processes (La/Y and Sr/Y) and $\delta^{18}O$ in plagioclase zones will be presented. Such correlations have not previously been observed in intra-crystal data from Iceland, and the implications that they have for $\delta^{18}O$ heterogeneity in the mantle source of basalts under Iceland will be explored.

SAMPLES

Geological and petrological context of the Borgarhraun flow, northern Iceland

The Theistareykir volcanic system in the Northern Volcanic Zone of Iceland is the most northerly on-land system in Iceland (Fig. 1). It has been described in detail by Slater (1996). It lies ~100 km north of the putative plume axis; this axis is possibly located at the NW of Vatnajökull (the icecap marked 'V' in Fig. 1) (e.g. Breddam, 2002), although a location ~50 km further south was preferred by Shorttle *et al.* (2010). Variability in major element, trace element and radiogenic isotope compositions of Theistareykir whole-rock samples and melt inclusions has been attributed to variation in mantle melt compositions, controlled both by source heterogeneity and the melting process under Theistareykir (Elliott *et al.*, 1991; Hémond *et al.*, 1993; Skovgaard *et al.*, 2001; Slater *et al.*, 2001; Maclennan *et al.*, 2003*b*; Stracke *et al.*, 2003*a*; Thirlwall *et al.*, 2004).

Borgarhraun is one of the early postglacial (12–7 ka BP) flows from Theistareykir, covering ~20 km^2, and is basaltic to picritic in composition (9·73–19·00 wt % MgO; Hémond *et al.*, 1993; Slater, 1996; Sigurdsson *et al.*, 2000). The flow, which is variably olivine-, plagioclase- and clinopyroxene-phyric, is shown in Fig. 1. It also contains gabbroic, wehrlitic, dunitic and troctolitic nodules up to ~2 cm in diameter. These nodules and the relationship of their constituent crystals to the host flow were described by Maclennan *et al.* (2003*a*). The variability in the trace element compositions of melt inclusions hosted by forsteritic olivines in the Borgarhraun flow is far greater than the variability observed amongst whole-rock samples from this flow (Slater *et al.*, 2001; Maclennan *et al.*, 2003*b*). Maclennan *et al.* (2003*a*) argued that this variability in melt inclusion chemistry represents some of the compositional variability of fractional melts sourced from different depths in the mantle melting region, and that the melts that crystallized the olivines mixed during crystallization

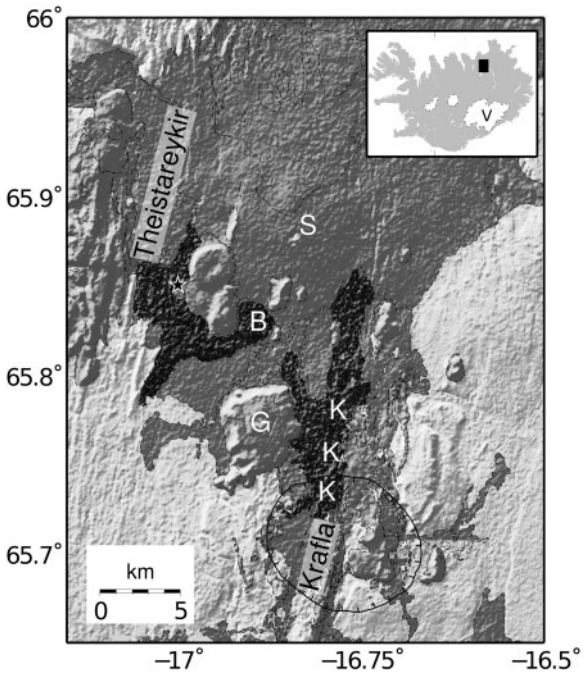

Fig. 1. Map of the Theistareykir and Krafla volcanic systems in northern Iceland; inset shows the location of the main map (black rectangle). Topography, illuminated from the NW, is from the most recent ASTER release (a product of METI and NASA, obtained from https://lpdaac.usgs.gov). Dark grey fill denotes eruptions from the last glacial and present interglacial (an interval of ≲100 kyr). Some sub-glacial tuyas and hyaloclastite ridges can be recognized by the illumination of their steep flanks. Lighter grey fill indicates older eruptions. The Borgarhraun eruption is shaded in black and has the letter 'B' at the approximate location of its eruptive vent. The black star marks the location at which samples from this study were collected. The Krafla Fires eruptions of 1975–1984 are also shaded black, with the letter 'K' repeated along the cone row that formed along the eruptive fissure. The summit of a large, early postglacial lava shield, Storaviti, is marked 'S'. The summit of Gaesafjoll, a large glacial eruption with a distinctive enriched composition, is marked 'G'. The axes of the Theistareykir and Krafla fissure swarms are labelled, with the illumination picking out the northwards and southwards continuation of those swarms away from the labels. The margin of the Krafla caldera is marked with a fine black line with tick marks on the downthrown interior.

to produce the whole-rock composition. It should be noted that in the present study the practice of Thomson & Maclennan (2013) is followed in using the purely descriptive term 'macrocryst' to define large crystals (~0·5–10 mm) in Icelandic basalts that are clearly distinguishable from the groundmass. This practice is followed, as opposed to using terms such as phenocryst or antecryst, to avoid implying a genetic relationship between the large crystals and their carrier basalt before the existence of any relationship—simple or complex—is established.

Sample collection, preparation and analyses

Sampling of gabbroic and wehrlitic nodules from the Borgarhraun flow was carried out in July 2007; all samples came from within a few tens of metres of 65°51·05′N, 16°59·93′W. Polycrystalline nodules containing plagioclase and large (up to ~1 cm diameter) plagioclase macrocrysts were made into 500 μm thick sections or mounted in epoxy resin. A mixture of macrocrysts and nodules were studied because Maclennan *et al.* (2003*a*) reported similar major element compositions for plagioclase crystals in the nodules and those existing as macrocrysts. Maclennan *et al.* (2003*a*) described in detail the petrography of the Borgarhraun nodules and macrocrysts, discussing the order of crystallization and noting that anorthitic plagioclase and high-Mg# clinopyroxene are found in nodules with forsteritic olivine and probably crystallized together from primitive melts. Zoning in plagioclase crystals was initially characterized by backscattered electron (BSE) imaging. Electron microprobe (EPMA) profiles of major element concentrations were then made across portions of the crystals that showed discrete, clear zones. Each of these zones was subsequently analysed by laser ablation inductively coupled plasma mass spectrometry (LA-ICP-MS) for trace element concentrations. SIMS trace element analyses were also performed in some of the narrower compositional zones. $^{18}O/^{16}O$ ratios were determined by SIMS in many of the same zones. Overall, 32 plagioclase zones in a total of 10 crystals were analysed for major and trace element concentrations and oxygen isotope ratios; nine crystals were from six polycrystalline nodules and the remaining crystal was a separate macrocryst. With the exception of nodule B9, none of the nodules described in the current study were ophitic.

The relationship between Borgarhraun plagioclase and ferromagnesian phases

In this section we document the evidence that anorthitic Borgarhraun plagioclase crystallized concurrently with forsteritic olivine and high-Mg# clinopyroxene, phases that are also present as macrocrysts and within polycrystalline nodules alongside the plagioclase crystals.

High-An plagioclase macrocrysts such as those found in Borgarhraun lavas are also known from elsewhere in Iceland; for instance, in depleted lavas and basaltic glasses from Kistufell, a sub-glacial table mountain in central Iceland (up to $An_{88·6}$; Breddam, 2002). Whereas the forsterite content of crystallizing olivine and the Mg# of crystallizing clinopyroxene generally decrease steadily as a magma evolves and the temperature of the crystallizing magma drops (e.g. Ford *et al.*, 1983; Beattie, 1993), the anorthite content of plagioclase is additionally dependent on the pH_2O of the melt (e.g. Yoder, 1965; Panjasawatwong *et al.*, 1995; Danyushevsky *et al.*, 1997; Putirka, 2005). Several pieces of evidence, however, strongly indicate that highly anorthitic Borgarhraun plagioclase [in this study up to 89·4 mol %; up to 91·0 mol % in the study by Maclennan *et al.* (2003*a*)] crystallized concurrently from primitive melts with high-Mg# clinopyroxene and

forsteritic olivine. First, these crystals are found in the same nodules as forsteritic olivines (up to Fo_{90}), and clinopyroxene with Mg# of up to ~92 (Maclennan *et al.*, 2003*a*). In one sample (gabbroic nodule B9), an idiomorphic $An_{87·6}$ plagioclase was found as a chadacryst within a Mg# 88·0 clinopyroxene [analysed by Winpenny & Maclennan (2011)]. Second, primitive MORB compositions not dissimilar to Borgarhraun, such as glass sample 527-1-1 from the FAMOUS segment of the Mid-Atlantic Ridge, may crystallize $An_{85–89}$ plagioclase (Bender *et al.*, 1978) by virtue of their low Na_2O contents and high CaO/Na_2O ratios [see Elthon & Casey (1985) and references therein]. Lastly, although some researchers have suggested that evolved melts (basaltic andesites to dacites; e.g. Lundstrom *et al.*, 2005; Lundstrom & Tepley, 2006) with moderate to high water contents (≥1·5 wt %; Danyushevsky *et al.*, 1997) may crystallize high-An plagioclase, pre-eruptive water contents for Borgarhraun melts are likely to be low (0·5 wt % H_2O; Saal *et al.*, 2002; Nichols & Wysoczanski, 2007).

The high anorthite contents of Borgarhraun plagioclase crystals are therefore likely to result from the crystallization of essentially anhydrous, primitive melts at the same time as high-Fo olivines and high-Mg# clinopyroxene crystals. These olivines and clinopyroxenes are known to preserve a record of compositional variability of mantle melts in their melt inclusions and compositional zones respectively (Maclennan *et al.*, 2003*a*; Winpenny & Maclennan, 2011). Consequently, it is feasible that high-An plagioclase zones may also preserve a record of the chemical and isotopic diversity of primary mantle melts.

Clinopyroxene–melt barometry has indicated that Borgarhraun clinopyroxene macrocrysts were formed at ~8 ± 2 kbar pressure (2σ range; Winpenny & Maclennan, 2011). The depth of plagioclase crystallization cannot be accurately assessed by barometry based on crystal–melt equilibria (Putirka, 2008), and can be best constrained from the presence of the $An_{87·6}$ plagioclase chadacryst in a Mg# 88·0 clinopyroxene. This clinopyroxene, and others from this nodule, gave crystallization pressures of around 7 kbar (Winpenny & Maclennan, 2011). Borgarhraun plagioclase crystallization is therefore likely to have occurred in the lower crust under Theistareykir.

ANALYTICAL METHODS

BSE images and electron microprobe analyses

BSE images of samples were obtained using a JEOL JSM-820 scanning electron microscope, with an accelerating voltage of 15 kV and beam current of 6–10 nA. Typical magnification was 35×, and images were assembled to produce composite views of entire nodules or macrocrysts. The concentrations of major and minor elements in plagioclase crystals, and also of several olivine macrocrysts in the polycrystalline nodules, were analysed on a Cameca SX100 electron microprobe at the Department of Earth Sciences, University of Cambridge, UK. Elements were analysed in wavelength-dispersive mode on five spectrometers, using an accelerating voltage of 15 kV and current of 10 nA for major elements or 100 nA for minor elements. The beam was focused to a 2 μm spot. Typical peak counting times were 20 s for major elements and 40 s for minor elements, and background counting times were 10 s. A set of natural silicate and metal standards was used at the start of each session for calibration of elemental concentrations, as follows: Na on jadeite, Mg on periclase, Si and Ca on diopside, Fe on fayalite, K on K-feldspar, Ti on rutile, Al on corundum, and Mn and Ni on pure metals. Analyses with oxide totals outside the range 98·5–101·5 wt % or poor stoichiometry were discarded. In general, internal precision from counting statistics for single analyses of elements present at >5 wt % is ~1% (1σ relative), 5% for elements at 1–5 wt % and up to 30% for elements present at <1 wt %.

Trace element analyses

Trace element concentrations were measured within the compositional zones recognized in BSE images. Analyses were performed by LA-ICP-MS at the University of Cambridge, and further analyses were made by SIMS at the Natural Environment Research Council (NERC) Ion Microprobe Facility, University of Edinburgh. Several zones were analysed by both LA-ICP-MS and SIMS, allowing comparison between elemental concentrations measured by the two techniques. There is good agreement (typically ~10% relative) between the concentrations of key trace elements measured by SIMS and LA-ICP-MS. Full data, including analyses of standards, are provided in Supplementary Data Electronic Appendix 1 (supplementary data are available for downloading at http://www.petrology.oxfordjournals.org).

LA-ICP-MS analyses

Elemental concentrations were measured using a New Wave UP213 Nd:YAG laser ablation system interfaced to a Perkin–Elmer Elan DRC II ICP-MS system. The laser repetition rate was 10 Hz and the laser power was ~5 J cm^{-2}. Spot diameter was 100–120 μm, and sample pit depth was around 50 μm. The ablation medium was helium gas. Data acquisition settings for the ICP-MS system were one sweep per reading, with 40 readings in one replicate, with a rinse-through time between analyses of 60 s. Dwell times were typically 10–50 ms, dependent on the concentration of each element. The CaO concentrations of the compositional zones, as determined from EPMA, were used for internal standardization of elemental concentrations. Intra-zone variability of these EPMA-determined CaO concentrations is negligible, with

standard errors on the means of repeat electron microprobe spot analyses consistently below 0·12 wt %. NIST SRM610 was used for calibration of elemental sensitivities, and accuracy was assessed by analysing NIST SRM612 and the glassed versions of international rock standards BIR1, BHVO-2 and BCR-2. Recovered values were typically 90–110% of published values (Jochum *et al.*, 2005; Jochum & Nehring, 2006). Repeat analyses of standard material did not indicate any systematic drift. For the elements analysed, matrix-matching of standards to unknowns for calibration of LA-ICP-MS signals is not generally considered necessary, as calibration using the NIST SRM610 glass typically produces concentrations with accuracies of 5–10% (reviewed by Pettke, 2006; Jochum & Stoll, 2008; Sylvester, 2008; see also Heinrich *et al.*, 2003). External precision was monitored throughout the analytical sessions by periodically making 4–10 repeat analyses on an in-house plagioclase standard (Beaver Bay anorthosite, Harker collection number 101377; see Carpenter *et al.*, 1985). The average 1σ external errors for each element across these groups of standard analyses are reported in Supplementary Data Electronic Appendix 1, and are used as the estimates of the precision of an analysis in the Borgarhraun plagioclase zones. This approach is considered reasonable as elemental variability amongst each set of repeat analyses in samples (typically three repeats) is, in most cases, within the ±2σ range determined from the repeat analyses on the standard. Data reduction was carried out using Glitter Software (GEMOC, Australia), which allows selection of signals, visualization of data quality and corrections for isobaric interferences. Errors reported in Electronic Appendix 1 are standard errors on the mean concentrations of elements in a recognized plagioclase zone.

SIMS analyses

SIMS analyses were performed using a Cameca IMS-4f ion microprobe, for which typical analytical procedures have been described by Shimizu & Hart (1982). Samples were gold coated and bombarded by a beam of O^- ions. The primary accelerating voltage was 10 kV, and the secondary ion accelerating voltage was 4·5 kV. A 75 V energy offset was used, with a 40 eV window, to suppress molecular ion interferences (Shimizu & Hart, 1982). Internal standardization was carried out using known Si concentrations from electron microprobe analyses. Spot size was ~25–35 μm, and the contrast aperture was set to 25 μm. Each analysis comprised 10 scans, each lasting ~2·5 min. Dwell times varied depending on elemental abundance, but ranged from 2 to 8 s per scan. Element abundances were calculated from secondary ion intensities (ratioed to ^{30}Si) using the in-house JCION-5 software. Molecular interferences (including REE oxide interferences) were corrected for in this software and further possible interferences were investigated with the aid of major element and LA-ICP-MS trace element concentrations. Accuracy was determined from daily analyses of the NIST SRM610 glass, and small corrections (<5%) have been applied to the data consistent with the daily SRM610 concentrations for each element. External precision was estimated using repeat analyses on the SHF-1 plagioclase (Irving & Frey, 1984). Individual correction factors were applied for each element of interest, which are based on comparisons of known ion yields (relative to ^{30}Si) for plagioclase standards with those of glass standards (Hinton, 1990). Precision, based on repeat analyses of the plagioclase standard, is generally ≤5%. Because of long analysis times, no repeat measurements were made in Borgarhraun plagioclase zones. The precision estimates and correction factors for each element are presented in Supplementary Data Electronic Appendix 1.

Oxygen isotope analyses

The $^{18}O/^{16}O$ ratios of compositional zones in plagioclase were determined by SIMS, using the Cameca IMS 1270 ion microprobe at the University of Edinburgh, in September–October 2010.

Sample preparation for $\delta^{18}O$ analyses

Plagioclase samples were cut out from their resin blocks or thick sections to remount them in Buehler EpoThin® resin. This remounting allowed reorientation of plagioclase crystals to move the areas of interest in each crystal closer to the centre of the sample mount, as required for high-precision O-isotope analysis by SIMS. Remounting was also necessary to reduce the total number of sample blocks in accordance with the available analytical time. Care was taken during remounting to preserve the previously studied surfaces, which contained information on the location of major and trace element variability within crystals. Laser ablation holes were filled with resin to provide as flat a surface as possible for SIMS analyses. Several plagioclase crystals were mounted along with grains of plagioclase standards ($An_{3·7}$, $An_{31·4}$, $An_{80·5}$ and $An_{89·6}$) within each sample block. One sample block was investigated per analytical session (equal to one day).

Analytical conditions

For the O-isotope analyses, the Cs^+ ion source was held at 10 kV, and the sample at −10 kV, resulting in a primary ion beam with a net impact energy of 20 keV. The primary beam current was 4 nA. The normal incidence electron gun was used for sample charge compensation. Pre-sputtering of the sampling area lasted ~60 s. The field aperture was set at 5000 μm and the entrance slit at 80 μm. The axial mass was ^{17}O, and ^{16}O and ^{18}O ions in the secondary beam were collected on the L'2 and H1 Faraday cups respectively. The mass resolving power, $M/\Delta M$, was 2400, at which there are no interferences on the ^{16}O and ^{18}O peaks. Yield and background for the Faraday cups were

calibrated at the start of each session. For each analysis spot, the overall $^{18}O/^{16}O$ ratio was calculated as the mean of 20 ratios (two blocks of 10 readings). Counting times during each reading were 5 s per mass, and count rates of ^{18}O were $\sim 10^7$ c.p.s. The $^{16}O^-$ secondary signal was centred in the field aperture by adjusting the primary beam L_4 deflection plate settings for every small (~1 mm by 1 mm) area of the sample surface where analyses were to be made. This method avoided the need for any large corrections to be made to the secondary ion beam trajectory from the dynamic transfer plates.

An important issue in obtaining good precision during measurements of oxygen isotopic ratios by ion microprobe is to ensure that the sample surface is as flat as possible. Analytical artefacts can be caused by deformation of the local electrostatic field close to areas with high relief. It was shown by Kita *et al.* (2009) that sample topography of 10 μm may elevate $\delta^{18}O$ values by 0·6‰, and topography of ~40 μm can increase values by as much as ~4‰. Analytical precision was also shown to be adversely affected by sample relief, with precision as poor as ±3‰ in the worst cases. For highly accurate and precise SIMS analyses of oxygen isotope ratios, Kita *et al.* concluded that polishing relief should be less than a few micrometres. Therefore, in preparing the sample mounts, hard polishing laps were used to minimize the development of relief during polishing. White light interferometry performed at the edges of the crystals that were embedded into the resin indicated that sample relief was minimal, and analyses were performed as far as possible from the filled laser ablation holes, typically a few hundred micrometres or more. During analyses of standard grains, larger grains were targeted, and rare grains that displayed a dark rim (indicating some relief) under the reflected light microscope of the IMS 1270 were avoided. Analyses were made within 8 mm of the centre of sample mounts so as to avoid disturbance to the electrostatic field close to the inside edge of the sample holder.

Analytical protocol, accuracy and precision

The full analytical protocol and raw $^{18}O/^{16}O$ data for each sample block are given in Supplementary Data Electronic Appendix 2 and summarized in Supplementary Fig. S1. Each of the three analytical sessions began with analyses on the plagioclase standards mounted in the sample blocks.

Instrumental drift during each analytical session was monitored by 'contiguous bracketing' of the analyses on unknowns with repeat measurements of grains of the $An_{31\cdot4}$ standard. Five analyses were performed on this standard after every 10–20 analyses on the Borgarhraun samples (see Supplementary Fig. S1). Mean values of each group of five analyses were used for establishing the drift corrections during each analytical session. A polynomial fit to the observed drift (as a function of analysis number) provided a good fit to the $An_{31\cdot4}$ standard data in the first analytical session, and linear fits in the other sessions. All corrections applied to the other standards and unknowns were made relative to the mean $^{18}O/^{16}O$ value of the group of five analyses on the $An_{31\cdot4}$ standard performed at the start of the analytical session. (See Supplementary Data Electronic Appendix 3 for details of the treatment of errors associated with the drift corrections.)

Precision on a single analysis of the samples was estimated from the typical standard deviation (1σ, external error) of repeat analyses on the $An_{31\cdot4}$ standard. As in previous SIMS oxygen isotope analyses (e.g. Eiler *et al.*, 2011), 1σ values from repeat analyses were found to be significantly greater than internal standard errors (1 SE) from counting statistics on a single analysis (the mean value of the standard error across all analyses in this study was 0·07‰). The mean 1σ of each batch of five analyses on the $An_{31\cdot4}$ standard was 0·12‰. This average precision is close to the average external precision (0·15‰, 1σ) calculated across sets of repeat analyses on olivine standards by Bindeman *et al.* (2008), and not too dissimilar to the value of ~0·2‰ (1σ) reported by Eiler *et al.* (2011) for the San Carlos olivine standard. In addition, it should be noted that the mean value of the standard deviations calculated for each group of 3–5 repeat analyses in the Borgarhraun plagioclase zones is very similar (0·10‰). Such precision in the samples is perhaps not unreasonable considering that homogeneity in $\delta^{18}O$ on the length scale of separation of the repeat analyses (~50 μm) is likely, given the diffusivity of oxygen in plagioclase (Farver, 2010).

Instrumental mass fractionation

Instrumental mass fractionation (IMF) of oxygen isotopes occurs during SIMS analysis of plagioclase on the IMS 1270 ion microprobe, leading to measured values of $\delta^{18}O$ that are several per mil away from true values. IMF is calculated as

$$\mathrm{IMF} = 10^3\left[\frac{(^{18}O/^{16}O_{\mathrm{measured}}) - (^{18}O/^{16}O_{\mathrm{true}})}{(^{18}O/^{16}O_{\mathrm{true}})}\right] \quad (1)$$

where $^{18}O/^{16}O_{\mathrm{measured}}$ is the SIMS-determined (drift-corrected) O-isotope ratio, and $^{18}O/^{16}O_{\mathrm{true}}$ is the ratio determined by laser fluorination. To make corrections for IMF it is necessary to determine the IMF values for standards with similar major element compositions to the samples.

Analyses of nine plagioclase standards for which $\delta^{18}O$ values are known from conventional (laser fluorination) determinations were made during two sessions in the days prior to the $^{18}O/^{16}O$ measurements on the Icelandic plagioclase samples (Fig. 2). Details of the standards used can be found in Supplementary Data Electronic Appendix 2. The results are in agreement with the finding of Coogan *et al.* (2007) that IMF varies linearly with anorthite (An, mol %) content of plagioclase. A small amount of scatter in

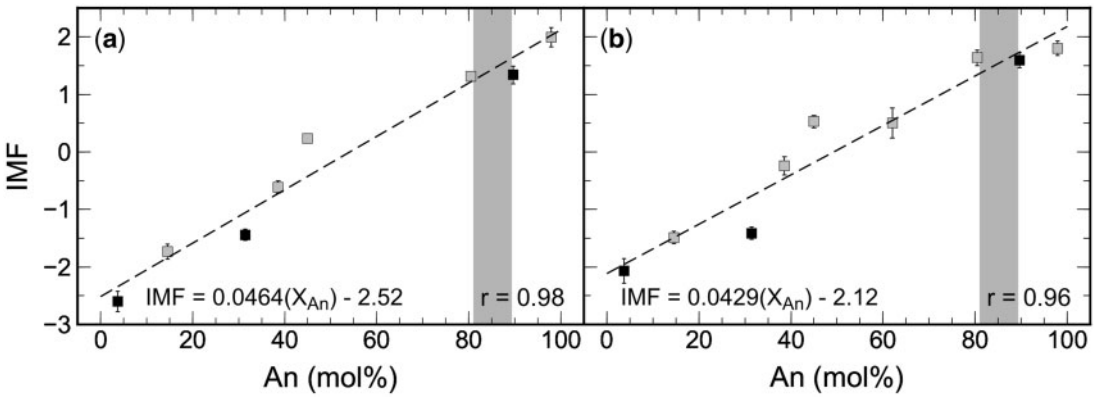

Fig. 2. Instrumental mass fractionation (IMF) vs anorthite (An) content of plagioclase for standards analysed during two analytical sessions, (a) and (b), in advance of the sessions for $^{18}O/^{16}O$ ratio determinations in the Borgarhraun plagioclase samples. Regression coefficients, *r*, of 0·98 and 0·96 confirm the trend observed by Coogan *et al.* (2007) that IMF increases linearly with plagioclase anorthite content. IMF is calculated from equation (1) (see text). The differences in slope and intercept of the regression lines between the two sessions demonstrate the need to determine IMF separately for each analytical session. The analyses shown in the plots were all performed on a separate epoxy block to the Borgarhraun plagioclase. Grains of three standards (those indicated in black) were mounted in each analysis block along with the unknowns (data for these standard grains can be found in Supplementary Data Electronic Appendix 2 and Fig. S1). The width of the grey shaded region shows the range of anorthite contents in Borgarhraun plagioclase samples. Error bars show ±1σ ranges from 5–10 repeat analyses in the same standards.

plagioclase standard data in the plots of IMF against anorthite content (Fig. 2) may result from small impurities (e.g. varying orthoclase content of the feldspar).

The IMF for each $^{18}O/^{16}O$ determination in the samples can therefore be corrected for using a scheme similar to that used by Coogan *et al.* (2007). For each analytical session, it was found that a suitable regression line for IMF versus anorthite content could be established by analysis of three of the standards in each block (3·7, 31·4 and 89·6 mol % anorthite; denoted by black squares in Fig. 2). It was suspected that grains of the fourth standard ($An_{80·5}$) were heterogeneous in $\delta^{18}O$. Different IMF versus anorthite regression lines were thus calculated for each analytical session. The IMF for each $^{18}O/^{16}O$ analysis in the plagioclase samples was calculated using the coefficients for each regression line and the anorthite content of each Borgarhraun plagioclase compositional zone. The variation in IMF over the range of anorthite contents in all the samples (~80–90 mol %) equates to an instrumentally induced variation in $\delta^{18}O$ of only ~0·5‰. It is also worth noting that varying the orientation of the plagioclase crystal lattice in the plane normal to the secondary ion beam has no measurable effect on the calculated value of IMF for a given plagioclase sample. This was confirmed by an investigation carried out by J. Craven on the Cameca IMS 1270 at Edinburgh in the week prior to the analyses of the Icelandic samples, by making repeat analyses on plagioclase standard material positioned in different crystallographic orientations.

$\delta^{18}O$ calculations and error propagation

After correcting for instrumental drift, $\delta^{18}O$ values of the Icelandic plagioclase samples were calculated from the measured $^{18}O/^{16}O$ ratios and corrected for IMF using the equation

$$\delta^{18}O = \frac{10^3}{(^{18}O/^{16}O_{VSMOW})}\left[\frac{(^{18}O/^{16}O_{measured})}{(IMF \times 10^{-3})+1} - (^{18}O/^{16}O_{VSMOW})\right] \quad (2)$$

where $^{18}O/^{16}O_{VSMOW}$ is the $^{18}O/^{16}O$ ratio of Vienna Standard Mean Ocean Water (VSMOW; equal to 0·0020052).

Within a single analytical session, where IMF is calculated from an IMF versus anorthite regression line, the precision of a $\delta^{18}O$ value calculated using equation (2) is dependent on: (1) the robustness of the drift correction; (2) the precision of the EMPA-derived anorthite content in a given compositional zone; (3) the robustness of the linear IMF–anorthite fit to the $^{18}O/^{16}O$ data from the standards; and (4) external analytical precision, as estimated from repeat analysis of the $An_{31·4}$ standard (0·12‰, 1σ, as described above). Propagation of these uncertainties through the drift corrections, IMF calculations and equation (2) was carried out by performing 2000 simulations of the corrections and calculations for each plagioclase zone. In each simulation the values for $\delta^{18}O$ and anorthite contents of samples and standards were drawn at random from appropriate distributions around mean values. Full details of the error propagation can be found in Supplementary Data Electronic Appendix 3.

The propagated 1σ errors mostly lie in the range 0·16–0·18‰. Overall, the largest contributions to the errors come from the external analytical precision and from uncertainty related to the drift corrections. Uncertainty resulting from the IMF corrections across the

dataset is relatively small, given the small range of anorthite contents in the samples; indeed, if a constant IMF value is used for all the sample zones, the $\delta^{18}O$ variability observed in the final dataset is affected to a negligible degree. With the exception of three compositional zones, the Borgarhraun plagioclase analyses were all conducted in the same analytical session, and the three zones analysed in the other sessions do not strongly influence the correlations presented below. Therefore any subtle offsets in $\delta^{18}O$ between analytical sessions would not affect the conclusions of this study.

Accuracy of dataset as a whole

Whereas the overall precision of the $\delta^{18}O$ values of plagioclase zones is in most cases 0·16–0·18‰ (1σ), the accuracy of the dataset as a whole (i.e. the amount by which the entire dataset may shift, without changing the magnitude of the $\delta^{18}O$ differences between points) is estimated to be a little poorer. Accuracy was assessed by considering the data plotted in Fig. 2a and b obtained during the two analysis sessions on standards. Regression lines were plotted for these two datasets using only the three standards that were used for daily determinations of the IMF versus anorthite relationship during the sample analysis sessions. From these lines, modelled $\delta^{18}O$ values of the remaining standards were then calculated using their known anorthite contents and measured $^{18}O/^{16}O$ ratios, which allowed calculation of the mismatch in $\delta^{18}O$ of each modelled value to that known from laser fluorination analyses. The mean mismatch across all remaining standards is 0·35‰, and therefore 0·4‰ is taken as an estimate of the accuracy of the dataset as a whole.

MAJOR AND TRACE ELEMENT, AND $\delta^{18}O$ ANALYSES OF PLAGIOCLASE COMPOSITONAL ZONES

Major element concentrations of single plagioclase compositional zones are reported in Table 2, together with selected trace element concentrations. The full dataset is given in Supplementary Data Electronic Appendix 1. The oxygen isotope data are also reported in Table 2.

The variability in plagioclase anorthite content [An, mol %; $An = 100X_{Ca}/(X_{Ca} + X_{Na})$, where X_i is the cation fraction of element i] matched the variation in greyscale intensity in BSE images, and compositional zones were identified accordingly. Anorthite contents of Borgarhraun plagioclase vary from 80·9 to 89·4 mol %. The anorthite content variation of the plagioclase crystals studied here is shown in Fig. 3, along with olivine forsterite contents and clinopyroxene Mg# data where these phases coexist with plagioclase in the nodules. Full olivine and clinopyroxene data for these nodules are given in Supplementary Data Electronic Appendix 4. The range of anorthite contents is similar to that observed in Borgarhraun nodules by Maclennan *et al.* (2003*a*). The variability of anorthite content in single crystals is $\lesssim$5 mol %.

Variability in trace element concentrations and $\delta^{18}O$ is observed between and within Borgarhraun plagioclase crystals. An overview of the range of trace element concentrations across all of the plagioclase compositional zones is shown in Fig. 4, where data points are shaded based on the anorthite content of the analysed zone. Variability in trace element concentrations and $\delta^{18}O$ in Borgarhraun plagioclase crystals is illustrated in Fig. 5a and b, along with the anorthite content variation across the crystals and BSE images of the analysed crystals. Intra- and inter-crystal variability in La and Sr concentrations and $\delta^{18}O$ is recognizable from Fig. 5. In general, inter-crystal variability in these indices in Borgarhraun plagioclase is greater than intra-crystal variability, but distinct variability is nonetheless preserved in some crystals, notably the plagioclase shown in Fig. 5b, which indicates that Borgarhraun plagioclase can preserve zonation in trace element concentrations and $\delta^{18}O$.

The following sections contain an investigation of the causes of variability in major and trace element concentrations in the plagioclase compositional zones, before discussion of the oxygen isotope data in further detail.

TRACE ELEMENT HETEROGENEITY IN AND BETWEEN PLAGIOCLASE CRYSTALS

Characterization of heterogeneity

Before making inferences about the compositions of the melts that crystallized the plagioclase zones, the textures of the crystals, the nature of zoning and chemical profiles must all be considered. Most compositional zones of Borgarhraun plagioclase crystals show sharp zoning in BSE images and some trace element variability between zones (Fig. 5). However, a small number of zones at the cores of three plagioclase crystals (B1.Pl, B16.Pl, B17.Pl) stand out as texturally different because of their very diffuse variation in greyscale intensity in BSE images over several hundred micrometres, reflecting gradational anorthite zonation across a portion of the crystal. Two of these three cores also display sieve textures (e.g. Fig. 6a). The majority of the interior of the crystal shown in Fig. 6b shows diffuse, poorly defined zoning, but a thin (~100 μm wide), ~An_{88} rim, sharply defined in the BSE image, surrounds the interior (this 'core' effectively extends across most of the diameter of the crystal). Core-forming zones in the two other plagioclase crystals are also, like the plagioclase in Fig. 6b, surrounded by thin, concentric, higher-An zones with sharp zoning in BSE images.

Table 2: Selected mean major and trace element and oxygen isotope data for Borgarhraun plagioclase compositional zones

Crystal	An	Mean concentration (wt %)							Mean concentration (ppm)						$\delta^{18}O_{plg}$	1σ
	(mol %)	SiO_2	Al_2O_3	FeO	MgO	CaO	Na_2O	Total	Ti	Sr	Y	Ba	La	Ce		
B1.P1.a	87·7	46·09	34·04	0·38	0·23	17·96	1·39	99·65	87·6	160·7	0·119	4·24	0·144	0·242	5·32	0·16
B1.P1.b.outer	n.d.	n.d.	n.d.	n.d.	n.d.	n.d.	n.d.	n.d.	n.d.	n.d.	n.d.	n.d.	n.d.	n.d.	5·02	0·16
B1.P1.b	83·5	47·05	32·92	0·45	0·24	16·96	1·85	99·39	214·5	232·4	0·131	12·58	0·704	1·069	4·06	0·16
B1.P1.c	82·5	47·33	32·73	0·43	0·22	16·70	1·96	99·23	211·8	252·2	0·137	16·26	0·585	1·002	4·13	0·16
B1.P1.d	84·8	46·46	33·39	0·42	0·19	17·04	1·69	99·24	169·9	262·7	0·194	14·39	0·513	0·889	4·17	0·15
B1.P1.e	86·6	46·13	33·54	0·42	0·17	17·54	1·51	99·43	154·9	268·2	0·193	14·54	0·408	0·753	4·15	0·16
B1.P1.f	87·9	45·74	33·95	0·40	0·15	17·86	1·36	99·96	112·6	273·3	0·186	11·90	0·256	0·443	4·13	0·16
B1.P1.g	86·3	46·28	33·63	0·41	0·17	17·50	1·53	100·70	94·2	266·6	0·160	9·69	0·180	0·295	4·21	0·16
B3b.P1.IP.a	88·7	45·79	33·91	0·33	0·23	18·18	1·28	99·94	48·0	97·3	0·084	0·84	0·037	0·068	5·66	0·16
B3b.P1.b	86·0	46·41	33·55	0·35	0·27	17·75	1·60	100·29	45·1	108·1	0·092	0·99	0·026	0·059	5·60	0·16
B3b.P1.IP.c	87·6	46·23	34·13	0·34	0·24	17·93	1·41	100·07	51·7	94·1	0·086	0·91	0·028	0·063	5·53	0·16
B3b.P1.d	86·3	46·60	33·64	0·35	0·27	17·64	1·55	99·36	83·8	114·4	0·106	1·22	0·027	0·077	5·66	0·16
B3b.P2.a	87·4	46·43	34·00	0·33	0·24	18·08	1·44	100·26	56·2	120·5	0·068	0·98	0·041	0·088	5·57	0·16
B3b.P2.IP.b	85·5	47·17	33·49	0·35	0·27	17·52	1·64	100·19	54·7	96·5	0·079	0·91	0·026	0·063	5·57	0·16
B3b.P2.IP.c	86·8	46·51	33·89	0·34	0·25	17·90	1·50	100·35	51·0	96·0	0·091	1·04	0·032	0·057	5·87	0·16
B3b.P2.d	85·7	46·79	33·54	0·34	0·27	17·57	1·62	99·98	72·9	123·2	0·065	1·12	0·026	0·070	5·72	0·16
B3b.P2.IP.e	86·2	46·61	33·32	0·34	0·27	17·84	1·58	99·88	56·1	97·6	0·090	1·19	0·029	0·068	5·67	0·16
B3b.P2.f	85·5	46·77	33·45	0·35	0·27	17·60	1·65	100·52	107·7	126·7	0·116	1·26	0·037	0·087	n.d.	n.d.
B4a.P1.	87·8	46·40	33·43	0·31	0·24	17·60	1·35	99·18	78·5	136·2	0·121	1·15	0·020	0·054	5·51	0·18
B4a.P2.	86·2	46·58	33·31	0·31	0·25	17·20	1·53	99·48	107·6	132·5	0·164	1·39	0·077	0·147	5·38	0·18
B9.P1.	87·5	46·14	33·62	0·34	0·21	17·52	1·38	99·25	n.d.	n.d.	n.d.	n.d.	n.d.	n.d.	n.d.	n.d.
B14.P1.	89·3	45·70	34·24	0·30	0·24	18·19	1·20	99·63	45·4	128·6	0·080	0·92	0·025	0·070	5·24	0·33
B14.P2.	n.d.	n.d.	n.d.	n.d.	n.d.	n.d.	n.d.	n.d.	115·8	140·4	0·082	1·41	0·020	0·093	n.d.	n.d.
B15.P1.a	86·8	45·99	33·70	0·35	0·23	17·59	1·47	98·38	77·7	165·9	0·082	3·47	0·077	0·169	4·54	0·16
B15.P1.b	87·1	45·96	33·56	0·37	0·23	17·57	1·44	99·56	114·1	194·6	0·055	4·45	0·104	0·192	n.d.	n.d.
B15.P1.IP.bA	87·7	45·35	33·45	0·34	0·22	17·63	1·37	99·15	67·7	140·4	0·088	3·12	0·074	0·162	5·23	0·16
B15.P1.c	83·7	47·00	33·04	0·40	0·27	16·95	1·82	99·80	117·3	212·5	n.d.	5·72	0·134	0·261	4·45	0·16
B15.P1.IP.cA	85·6	46·39	33·43	0·36	0·24	17·26	1·60	99·56	55·8	161·9	0·063	3·87	0·103	0·196	n.d.	n.d.

Crystal	An	Mean concentration (wt %)							Mean concentration (ppm)						$\delta^{18}O_{plg}$	1σ
	(mol %)	SiO_2	Al_2O_3	FeO	MgO	CaO	Na_2O	Total	Ti	Sr	Y	Ba	La	Ce		
B15.P2.a	85·9	46·44	33·63	0·37	0·24	17·55	1·60	100·13	107·6	162·8	0·073	3·58	0·075	0·175	4·54	0·16
B15.P2.IP.aA	85·6	46·58	33·52	0·37	0·24	17·57	1·64	99·88	69·8	131·4	0·081	2·83	0·076	0·153	n.d.	n.d.
B15.P2.b	86·4	46·32	33·70	0·37	0·23	17·62	1·54	100·02	99·5	181·6	0·073	3·76	0·088	0·178	n.d.	n.d.
B15.P2.IP.aB	86·6	46·29	33·74	0·36	0·23	17·69	1·51	99·93	70·9	137·4	0·087	2·80	0·080	0·162	4·90	0·16
B15.P2.c	84·1	46·84	33·20	0·40	0·26	17·24	1·80	98·85	73·5	198·3	0·064	4·65	0·088	0·182	4·67	0·16
B16.P1.IP.aa	88·0	46·14	33·79	0·28	0·25	17·72	1·34	99·77	46·0	98·0	0·071	1·16	0·025	0·078	n.d.	n.d.
B16.P1.IP.a	89·2	45·95	34·15	0·31	0·25	18·08	1·22	99·53	40·5	96·2	0·067	1·07	0·024	0·059	5·11	0·16
B16.P1.b	87·8	46·06	33·92	0·29	0·25	17·80	1·36	99·34	89·3	126·7	0·054	1·64	0·060	0·096	5·12	0·16
B16.P1.IP.c	88·4	46·99	33·70	0·31	0·24	18·01	1·31	100·21	48·0	103·0	0·072	1·41	0·038	0·079	n.d.	n.d.
B16.P1.d	87·9	46·80	33·76	0·32	0·24	17·83	1·36	100·09	77·1	134·9	0·052	1·56	0·037	0·081	n.d.	n.d.
B16.P1.IP.e	89·4	46·40	33·96	0·34	0·22	18·18	1·19	99·87	48·9	108·1	0·078	1·59	0·037	0·082	4·98	0·16
B16.P1.IP.f	88·0	46·34	33·37	0·32	0·24	17·64	1·33	100·18	49·4	118·3	0·072	2·06	0·044	0·090	4·90	0·16
B16.P1.g	84·8	46·94	33·19	0·36	0·26	17·23	1·71	100·11	266·9	249·0	0·144	13·81	0·437	0·848	4·13	0·16
B17.P1.a	84·8	47·31	33·00	0·34	0·27	17·43	1·73	101·06	126·0	223·3	0·104	4·24	0·086	0·178	4·84	0·16
B17.P1.b	80·9	47·95	32·58	0·40	0·25	16·65	2·18	99·96	302·8	276·3	0·156	13·04	0·904	1·463	4·22	0·16
B17.P2.	88·4	45·62	33·62	0·32	0·21	18·06	1·31	100·09	20·4	144·2	0·149	n.d.	0·061	0·108	n.d.	n.d.

Zone codes mostly follow the format B*xx*.P*y*.*zz* where *xx* is the nodule, *y* is the crystal number in a nodule and *zz* is the zone code. n.d., not determined. Some codes include an additional 'IP' before the zone number, indicating that trace elements were determined by SIMS rather than LA-IPC-MS. B17.P1 and B17.P2 are separate macrocrysts, rather than being from the same polycrystalline nodule. $\delta^{18}O$ data are reported as plagioclase values ($\delta^{18}O_{plg}$; IMF- and drift-corrected); 1σ errors presented for $\delta^{18}O$ data are based on analyses in the plagioclase zones ($n = 3$–5); the stated errors are based on standard errors of the means of repeat analyses, but with errors propagated from the drift and IMF corrections (see Electronic Appendix 3). The full dataset, including errors on major and trace element determinations for each compositional zone, are tabulated in full in Electronic Appendix 1.

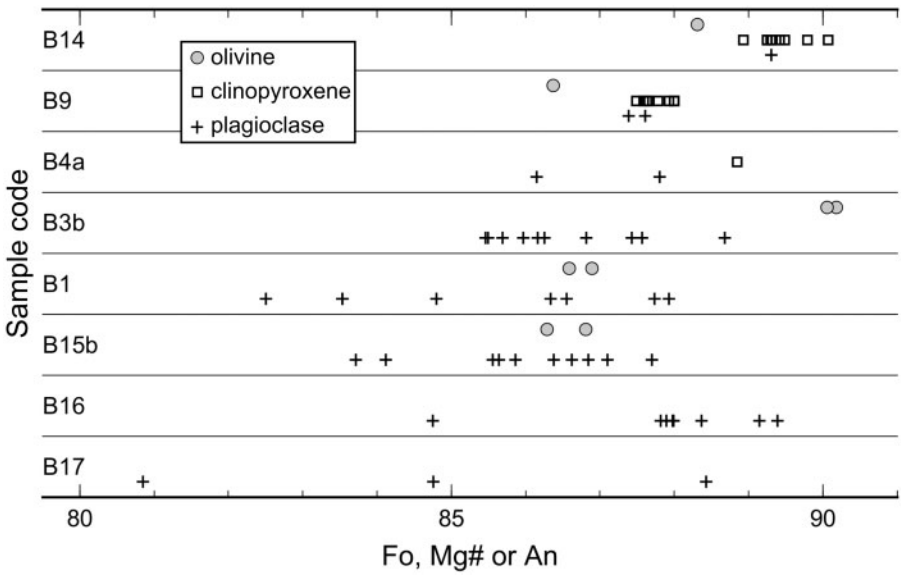

Fig. 3. Forsterite and anorthite contents and Mg# of olivine, plagioclase and clinopyroxene (respectively) in polycrystalline nodules and macrocrysts from the Borgarhraun flow. Clinopyroxene data are from Winpenny & Maclennan (2011). Full major element compositions of all phases can be found in Table 2 and Supplementary Data Electronic Appendices 1 and 4. Grey circles represent olivine forsterite contents, open black squares are clinopyroxene Mg# values and black crosses are plagioclase anorthite contents. Different points typically show compositions of single compositional zones; not every crystal in each nodule was analysed. The mineralogy of Borgarhraun nodules and distribution of crystal compositions are similar to those observed by Maclennan *et al.* (2003*a*).

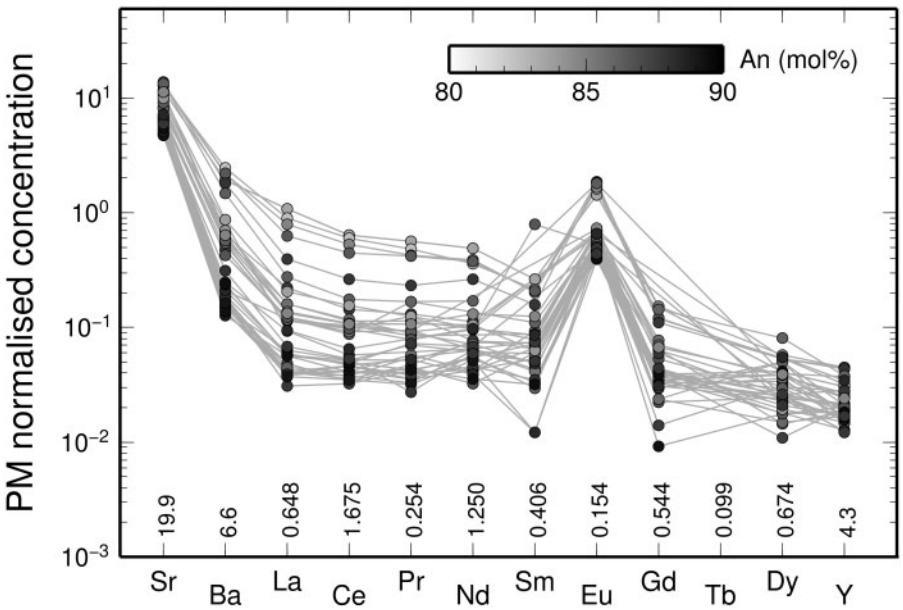

Fig. 4. Trace element concentrations of Borgarhraun plagioclase crystal compositional zones, shaded by anorthite content of the zone. Normalizing values, shown in the bottom of the plot, are from McDonough & Sun (1995). Data are a mixture of LA-ICP-MS and SIMS data.

Notably, all three cores appear to have been partially resorbed, perhaps by the high-CaO/Na_2O melts that then crystallized the rims.

Because significant CaAl–NaSi diffusion has seemingly occurred in the bulk of the crystal, incompatible trace elements will have significantly diffused in these zones. Indeed, when concentrations of Sr, La and Y in this group of texturally distinct plagioclase zones are compared with concentrations in the rest of the Borgarhraun plagioclase zones (Fig. 7a and b), it is evident that the former concentrations are generally higher, and in the plot of La versus Sr this group of zones appears to lie on a trend distinct

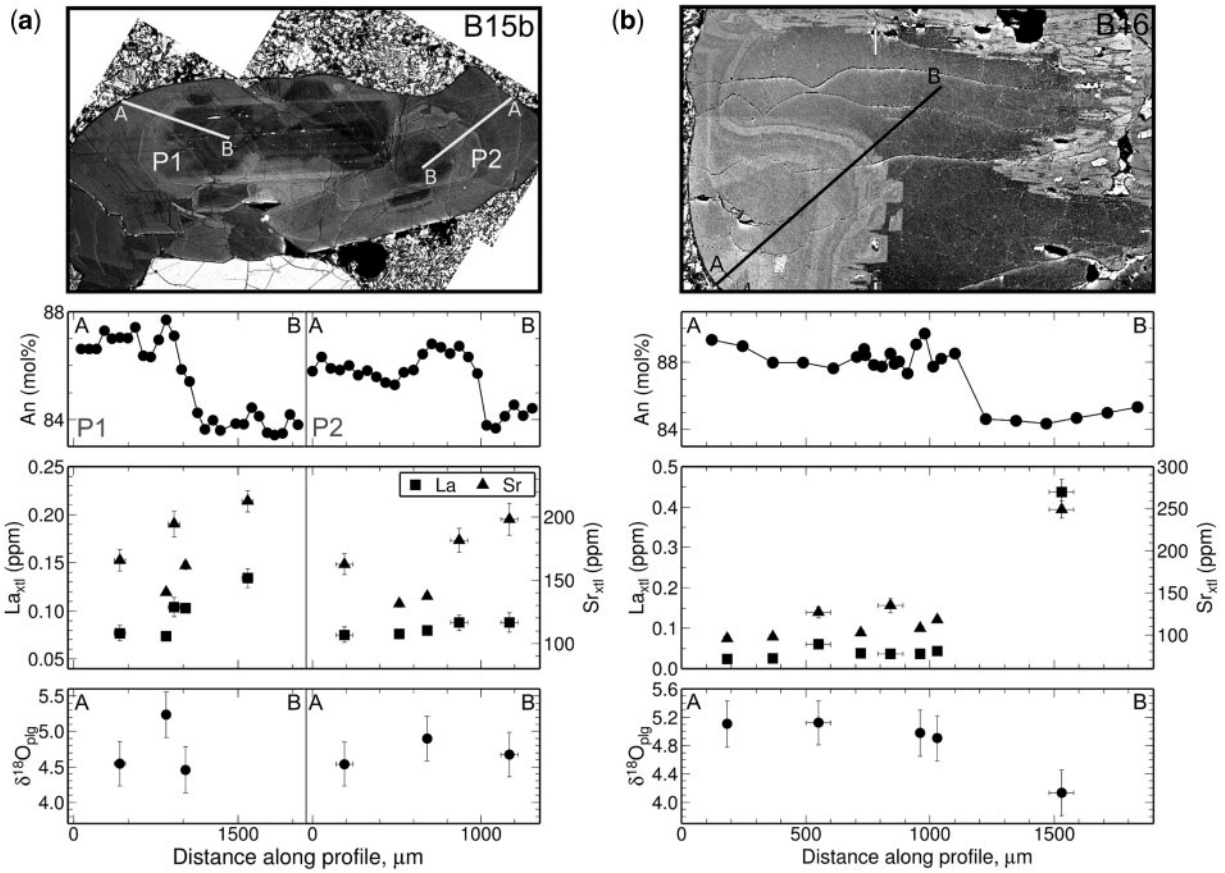

Fig. 5. Chemical and isotopic profiles across Borgarhraun plagioclase crystals (a) Bl5b.P1 and Bl5b.P2, and (b) Bl6, between the points A and B as marked on each image. The images show BSE greyscale intensity variation, primarily reflecting variation in anorthite content (top set of plots). Lower graphs show crystal La and Sr concentrations for several of the compositional zones identified in the BSE images. The vertical error bars show ±2σ ranges in the case of single analyses, or ±2 standard error ranges where the means of repeat analyses are plotted. The full width of the horizontal error bars demonstrates the typical size of the analytical spot: 100 μm wide for LA-ICP-MS spots and 25 μm wide for SIMS spots. $\delta^{18}O$ determinations of plagioclase $\delta^{18}O_{plg}$ are shown in the lowermost plots, with vertical bars showing propagated ±2σ error ranges.

from that of the rest of the data (open versus closed symbols in Fig. 7a and b). Because both the trace element concentrations and textures of this group of plagioclase zones are similar to each other, but distinct from those of the other Borgarhraun plagioclase zones, it is considered necessary to treat these plagioclase zones as a separate group.

Melt compositional heterogeneity as the cause of trace element heterogeneity in crystals

Across all Borgarhraun plagioclase compositional zones, the range in La concentrations is 0·020–0·904 ppm. In Sr and Y, ranges are 94·1–276·3 ppm and 0·053–0·194 ppm respectively. Excluding the group of resorbed cores, the ranges in La, Sr and Y are 0·020–0·144 ppm, 94·1–194·6 ppm and 0·053–0·164 ppm respectively; the corresponding ranges of crystal La/Y and Sr/Y ratios are 0·17–1·89 and 808–3540. These ranges are too large to be caused by melt evolution during fractional crystallization alone.

The variability observed in Borgarhraun plagioclase trace element concentrations may result from compositional heterogeneity in the melts that crystallize under Theistareykir. This conclusion was established for Borgarhraun clinopyroxene compositional zones by Winpenny & Maclennan (2011); the next few paragraphs follow a similar line of investigation to that used for the clinopyroxene compositions.

First, it is necessary to establish whether or not variability in plagioclase–melt partition coefficients (*D* values) alone could cause the variability observed amongst the crystals. Partition coefficients largely depend on the anorthite content of plagioclase and the temperature of crystallization (Blundy & Wood, 1994; Bindeman *et al.*, 1998; Bédard, 2006). The range of temperatures of early plagioclase crystallization for Borgarhraun melts is likely to be ≲60°C (the ±2σ range across all crystal–melt

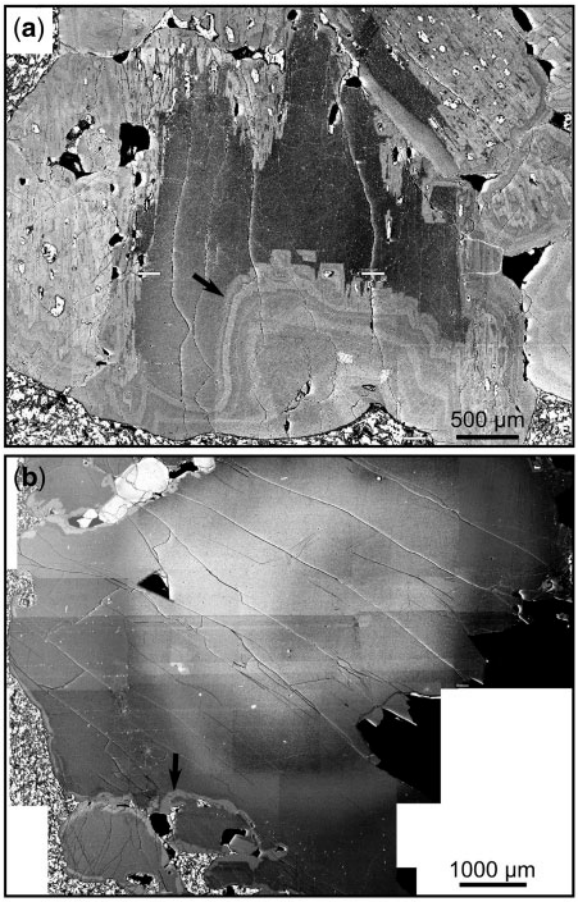

Fig. 6. Composite BSE images of two of the three large plagioclase crystals that have resorbed cores, (a) Bl6.P1 and (b) Bl.P1. The black arrows in each image indicate the outer margin of the resorbed core, at the point at which each core is mantled by rim zones, which typically have higher anorthite contents (indicated by lighter greyscale tones) than the core zones. Noteworthy features are the sieve textures in and around the dark-coloured resorbed core in (a), and the diffuse anorthite zoning in the core of (b). As well as being texturally distinct, the resorbed core zones have distinct trace element concentrations (see Fig. 7a and b).

equilibrium pairs for clinopyroxene–melt thermobarometry is 56°C; Winpenny & Maclennan, 2011). By using appropriate equations for calculating partition coefficients (see Supplementary Data Electronic Appendix 5), it is observed that the full range of anorthite contents in Borgarhraun plagioclase affects Sr, Y and La partition coefficients by only <13%, <10% and <2% (respectively) relative to the smallest D values. Varying temperature from 1200 to 1260°C changes mean D_{La}, D_Y and D_{Sr} for Borgarhraun plagioclase in the range 0·078–0·054, 0·0088–0·0100 and 1·69–1·60, respectively. Therefore partition coefficient variability, caused by the varying anorthite content of plagioclase or by uncertainties in crystallization temperature, is not capable of causing the roughly sevenfold variability in La, the two- to three-fold variability in Y and Sr concentrations, and similarly large ranges of La/Y and Sr/Y ratios in Borgarhraun plagioclase.

A second possibility is that variable growth rates in plagioclase may be capable of creating the large range in trace element concentrations. At very fast growth rates, non-equilibrium partitioning may prevail, as a chemical species is not able to diffuse fast enough in or out of a chemical boundary layer immediately adjacent to the growing crystal. It was noted by Winpenny & Maclennan (2011), however, that extremely rapid growth rates of clinopyroxene seen in experiments do not cause significant fractionation of the REE with respect to each other, and so variation in Borgarhraun clinopyroxene growth rates could not explain the observed range of crystal Ce/Yb ratios. Because rates of diffusion of REE and Y are similar in plagioclase, and plagioclase co-crystallized with clinopyroxene from the same melt, it is unlikely that variation in growth rates could explain the ranges of trace element compositions. Furthermore, a conclusion of the parameterization of Watson (1996) was that melts with temperatures in excess of 1000°C are generally immune to lattice entrapment of trace elements at natural growth rates. Another observation is that La, Sr and Y concentrations in some of the smallest plagioclase crystals (<500 μm diameter; e.g. crystals Bl4.P1 and Bl4.P2) are among the lowest concentrations observed. This observation is in contrast to the suggestions of Albarède & Bottinga (1972) that small crystals may display high concentrations of incompatible trace elements as a result of high nucleation density and rapid crystal growth rates, coupled with relatively sluggish diffusion of the trace elements in the surrounding melt.

Neither the variable growth rates of plagioclase crystals nor variation in crystal–melt partition coefficients are thus considered important in creating the variability in trace element concentrations and ratios in the Borgarhraun plagioclase. Compositional heterogeneity of the crystallizing melts is therefore the preferred explanation for the variability in crystal trace element concentrations and ratios.

TRACE ELEMENT VARIABILITY OF MELTS IN EQUILIBRIUM WITH PLAGIOCLASE

Potential origins of melt trace element variability

As it is now established that variability in plagioclase trace element concentrations and ratios primarily reflects the diversity of compositions of crystallizing melts, and that Borgarhraun plagioclase co-crystallized with forsteritic olivine and high-Mg# clinopyroxene, it is desirable to investigate whether Borgarhraun plagioclase preserves a record of the compositional heterogeneity of primary mantle melts, in a similar manner to the records preserved

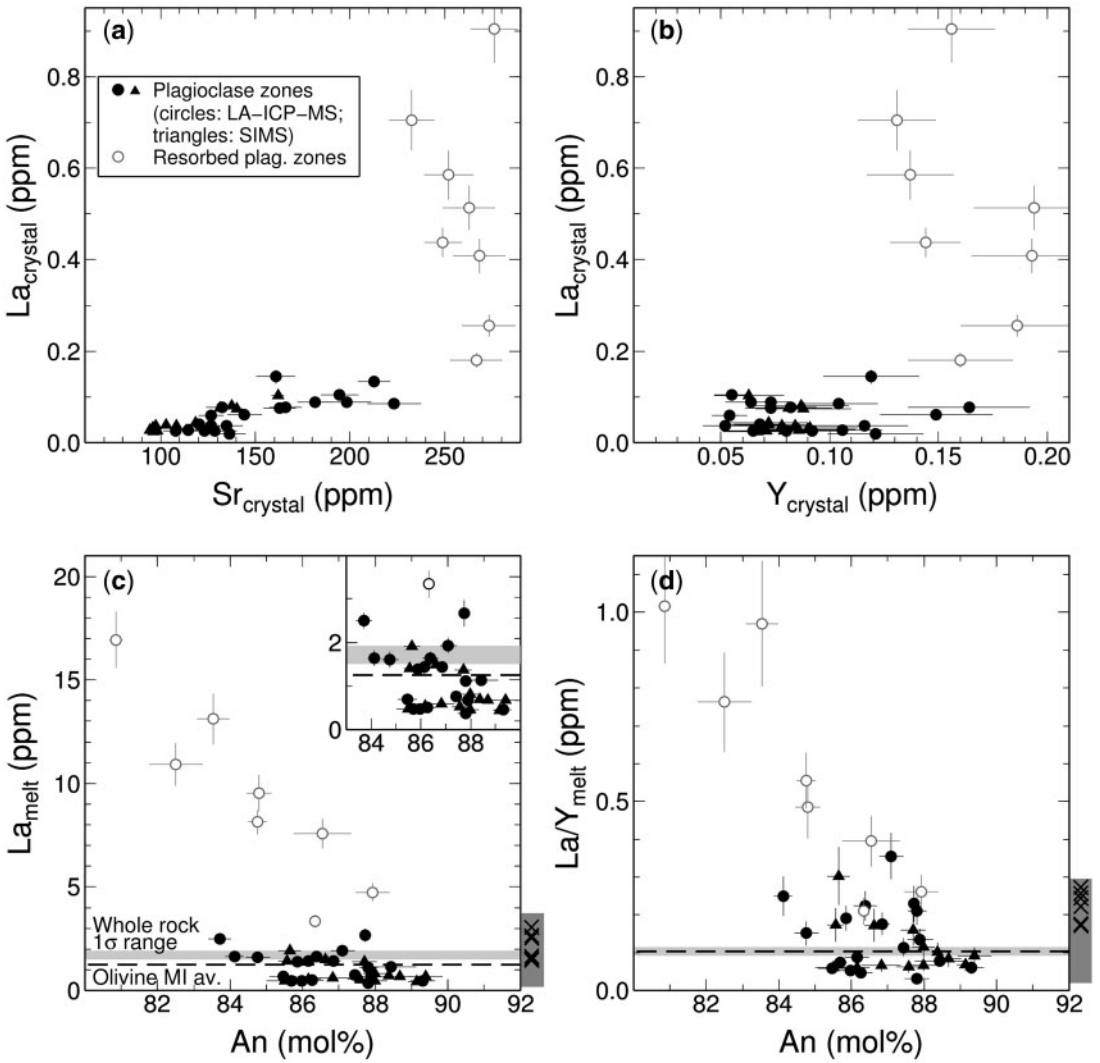

Fig. 7. (a, b) Trace element concentrations of Borgarhraun plagioclase compositional zones. Open symbols are zones identified as resorbed cores; filled symbols are the remaining zones. In (a), the resorbed cores form an array with high La and high, roughly constant Sr. The compositions of the remaining zones define a positive correlation between La and Sr with $r = 0{\cdot}78$. In (b), the resorbed cores have, in general, higher Y concentrations than the remainder of the zones. In (c) and (d), trace element indices of the melts calculated to be in equilibrium with plagioclase compositional zones are plotted versus zone anorthite content (for partition coefficient calculations see Supplementary Data Electronic Appendix 5). The inset in (c) shows an enlargement of compositional zones with La <4 ppm. The light grey fields in (c) and (d) indicate the 1σ range of La or La/Y in Borgarhraun whole-rock samples (Elliott *et al.*, 1991; Hémond *et al.*, 1993; Slater, 1996; Maclennan *et al.*, 2003*b*). Average Borgarhraun olivine-hosted melt inclusion compositions are shown in (c) and (d) as black dashed lines. Dark grey fields on the right of (c) and (d) indicate the ranges of olivine-hosted melt inclusions (see Maclennan *et al.*, 2003*a*); the black crosses mark the seven La and six La/Y data points from plagioclase-hosted melt inclusions from Slater (1996) (these ratios are not plotted against an anorthite content as no information exists on crystal zonation). Error bars in all plots show 2σ ranges.

in these co-crystallized phases (Slater *et al.*, 2001; Maclennan *et al.*, 2003*a*, 2003*b*; Winpenny & Maclennan, 2011).

To establish whether or not the melt compositional variability recorded in the plagioclase zones reflects the range of compositions generated by fractional melting of the mantle, or instead reflects the influence of crustal processes [e.g. assimilation–fractional crystallization (AFC) or dissolution–reaction–mixing (DRM) mechanisms], Sr, Y and La concentrations of melts in equilibrium with Borgarhraun plagioclase zones have been calculated using a suitable crystal–liquid partition coefficient for each element and zone (mean values of the coefficients are given in Table 3; separate values for each zone are given in Supplementary Data Electronic Appendix 1). The calculation of partition coefficients for each zone is based on the anorthite content of that zone, and reflects as closely as possible the conditions of crystallization, using a

Table 3: Mean values of partition coefficients used for calculation of trace element indices of melts in equilibrium with Borgarhraun plagioclase compositional zones

Element	D_i	2σ
Sr	1·58	0·07
Y	0·0101	0·0003
La	0·0539	0·0002

Further details on partition coefficient values are given in Electronic Appendix 5. It should be noted that the spread of D values, shown by the 2σ ranges, is small, owing to the narrow range of anorthite contents of the Borgarhraun plagioclase zones (<10 mol %).

temperature of 1260°C (Maclennan *et al.*, 2003*a*; Winpenny & Maclennan, 2011). Full details of the partition coefficient calculations are given in Supplementary Data Electronic Appendix 5.

The ranges of La, Sr and Y concentrations in the melts calculated to be in equilibrium with Borgarhraun plagioclase are 0·37–16·93 ppm, 59·6–175·5 ppm and 5·08–19·70 ppm, respectively. The corresponding ranges of La/Y and Sr/Y ratios are 0·03–1·02 and 5·04–22·71 respectively. Excluding the resorbed cores, the ranges for La, Sr and Y are 0·37–2·67 ppm, 59·6–136·2 ppm and 5·08–16·38 ppm respectively, and the ranges of La/Y and Sr/Y ratios are 0·03–0·36 and 5·04–22·71 respectively. Again, it is worth stating that these large ranges cannot be explained by fractional crystallization or uncertainties in partition coefficients (as discussed in the previous section).

It was argued by Maclennan *et al.* (2003*a*) that AFC and DRM processes do not play a role in controlling the trace element systematics of Borgarhraun olivine-hosted melt inclusions, and by Winpenny & Maclennan (2011) that these processes do not control the range of compositions of melts in equilibrium with Borgarhraun clinopyroxene. Because most Borgarhraun plagioclase crystals are inferred to have crystallized concurrently with high-Fo olivines and high-Mg# clinopyroxene, it is unlikely that AFC or DRM mechanisms have played a significant role in controlling the trace element chemistry of the melts that crystallized most of the plagioclase zones. Nevertheless, we initially consider the possible role of assimilation mechanisms by examining the covariance in the plagioclase trace element compositions.

DRM mechanisms may have played a minor role in the history of Borgarhraun plagioclase, as the textures of the group of resorbed cores discussed above indicate that some dissolution of plagioclase has occurred. Such dissolution could plausibly elevate Sr/Y ratios in some melts (Danyushevsky *et al.*, 2003), but whereas the range in equilibrium melt Sr/Y could possibly be explained by plagioclase dissolution, the variability in La/Y ratios of the equilibrium melts cannot be explained by this mechanism. The reasoning is essentially identical to that given by Winpenny & Maclennan (2011) with regard to clinopyroxene (where it was shown that the variability in melt Ce/Yb ratios could not be explained by DRM mechanisms), because REE and Y concentrations in Icelandic plagioclase crystals are too low to significantly influence melt light REE to heavy REE (LREE/HREE) and LREE/Y ratios by their dissolution.

The large variability in trace element concentrations and ratios in the melts in equilibrium with plagioclase zones may well reflect some of the variability in mantle melt compositions. Under Theistareykir, the diversity of melt compositions is thought to be homogenized by mixing in the lower crust while fractional crystallization progresses (Maclennan *et al.*, 2003*a*). The equilibrium melt data will be investigated further in the following sections.

Comparisons with literature data

La concentrations and La/Y ratios of melts in equilibrium with plagioclase compositional zones are plotted in Fig. 7b and d versus the anorthite content of each zone. Also shown are the 1σ ranges of compositions of Borgarhraun whole-rock data (light grey fields) and the mean values of olivine-hosted melt inclusions (dashed lines). The group of resorbed Borgarhraun plagioclase cores is distinguished from the rest of the data (open versus filled symbols).

First, it is notable in Fig. 7b and d that the melts in equilibrium with resorbed cores typically have higher La and La/Y than melts in equilibrium with other compositional zones. In the case of La concentrations (Fig. 7b), the trend of the resorbed core data is towards low-An compositions and high La concentrations. A similar pattern is observed for La/Y in Fig. 7d. These observations suggest that the cores may have crystallized from or diffusively re-equilibrated with more evolved, high-La and -La/Y melts with relatively low CaO/Na_2O. It is difficult with the current dataset to explain fully the chemistry of the resorbed cores, particularly as the trace element concentrations and anorthite contents of the crystals may have become decoupled by diffusion, which has clearly occurred in at least one resorbed core (as shown by diffuse anorthite zonation in the crystal in Fig. 6b). Nevertheless, the resorbed core data show that some evolved, high-La and high-La/Y melt is likely to have been present in the Theistareykir system (e.g. Eiler *et al.*, 2000*a*), perhaps as an interstitial melt in a mush zone.

Amongst the melts in equilibrium with the rest of the plagioclase zones, the La concentrations and La/Y ratios of the zones show significant variability at $\sim An_{86-90}$;

there is also variability in Sr/Y. This trace element variability in anorthitic plagioclase is similar to the variability in LREE/HREE seen in melt inclusions in forsteritic olivines from Borgarhraun (Slater *et al.*, 2001; Maclennan *et al.*, 2003*a*, 2003*b*). Maclennan *et al.* (2003*a*) showed that this melt inclusion variability is greatest at $\sim Fo_{90}$, and the range in LREE/HREE ratios diminishes while the forsterite content of the host olivine decreases, a pattern that those researchers suggested was created by melt mixing occurring concurrently with fractional crystallization. Because of the similarity of the mean melt inclusion composition to the whole-rock composition of the host basalt, the Borgarhraun whole-rock composition was interpreted by Maclennan *et al.* (2003*a*) to represent a final 'mixed' melt composition. The distribution of olivine-hosted melt inclusion trace element data was used to suggest that mantle melt mixing was completed by the time the melts were crystallizing $\sim Fo_{86}$ olivines.

The variability in plagioclase equilibrium melt trace element ratios at high anorthite contents in Fig. 7c and d mimics the spreads of LREE/HREE ratios of olivine-hosted melt inclusions in high-Fo olivines from Maclennan *et al.* (2003*a*) and of high-Mg# clinopyroxene equilibrium liquids from Winpenny & Maclennan (2011). These ranges have been ascribed by those researchers to mantle melt compositional variability. The similarities between the distributions of trace element indices for melts associated with these three phases mean that anorthitic plagioclase crystals from Borgarhraun may also provide a record of the compositional diversity of fractional mantle melts. The ranges of La and La/Y in olivine-hosted melt inclusions analysed by Slater *et al.* (2001) and Maclennan *et al.* (2003*b*) are shown in Fig. 7b and d as vertical dark grey fields; Borgarhraun plagioclase-hosted melt inclusions analysed by Slater (1996) are also shown to highlight the parallels in variability of melt compositions. However, detailed quantitative comparisons between the melt inclusion and equilibrium melt datasets should not be attempted. This is because of the inaccuracies inherent in calculating trace element concentrations and ratios of the equilibrium melts (arising in part from a lack of existing high-pressure data for plagioclase–melt trace element partitioning; see Supplementary Data Electronic Appendix 5). It should be noted that, irrespective of these inaccuracies (which would apply to each trace element dataset as a whole; that is, causing the same proportional shift to each calculated value), the existence of variability in the equilibrium melt data—the key observation—for each of the trace element indices is robust.

Mantle and crustal influences in equilibrium melt trace element correlations

La concentrations in the melts in equilibrium with all plagioclase zones are plotted against the Sr concentrations in the same melts in Fig. 8a. Apart from the resorbed cores, the equilibrium melts show a positive correlation between La and Sr ($r = 0{\cdot}81$). A positive correlation is also apparent in the olivine-hosted melt inclusion data of Maclennan *et al.* (2003*a*) ($r = 0{\cdot}74$); these data are plotted for comparison. Although part of the correlation between La and Sr can be explained by crystallization of olivine ± clinopyroxene (fine black lines labelled 'ol' and 'cpx' in Fig. 8a), very large extents of crystallization would be required, which is not consistent with the primitive compositions of olivine and plagioclase crystals. Fractional mantle melting, however, is capable of producing these ranges in La and Sr concentrations, with melts produced in the presence of garnet being the most enriched in La and Sr (Hauri *et al.*, 1994).

In a similar manner to the crystal chemical data shown in Fig. 7a, the trend in La and Sr of the melts in equilibrium with the resorbed plagioclase cores in Fig. 8a is almost orthogonal to the trend of the rest of the plagioclase zones. The trend towards higher La concentrations at roughly constant or slightly decreasing Sr concentrations may be consistent with the resorbed cores having crystallized from or re-equilibrated with a basaltic melt that has been contaminated by silicic partial melts of basaltic crust. Such a process cannot account for the positive correlation in the rest of the plagioclase data, as partial melts of crust will be relatively La-rich but Sr-poor, as a result of the compatibility of Sr in crustal plagioclase (Jónasson, 1994; Bédard, 2006).

La/Y versus Sr/Y ratios of equilibrium melts and melt inclusions are plotted in Fig. 8b. La/Y is influenced little by moderate degrees of fractional crystallization, whereas Sr/Y would decrease slightly during gabbro crystallization owing to the compatibility of Sr in plagioclase. Again, excepting the resorbed cores, a positive correlation ($r = 0{\cdot}83$; shown in Fig. 8d) can be observed between these indices in the plagioclase equilibrium melts, which is similar to the positive correlation ($r = 0{\cdot}77$; see Fig. 8c) seen in the olivine-hosted melt inclusions. The correlation for the plagioclase data cannot be explained by dissolution of plagioclase, which would serve to increase Sr/Y at nearly constant La/Y, or fractional crystallization, which would also have a negligible effect on La/Y. It should be noted that the positive correlations between La and Sr, and between La/Y and Sr/Y in the equilibrium melt data hold true even if calculated partition coefficients for La, Sr or Y contain systematic inaccuracies (described in Supplementary Data Electronic Appendix 5), as relative variability in these indices is robust. Such inaccuracies, essentially affecting each equilibrium melt datum point by the same proportion, may well explain why the plagioclase equilibrium melt data do not exactly match the ranges of olivine-hosted melt inclusion data in Fig. 8. However, this misfit does not affect the observation of the good positive

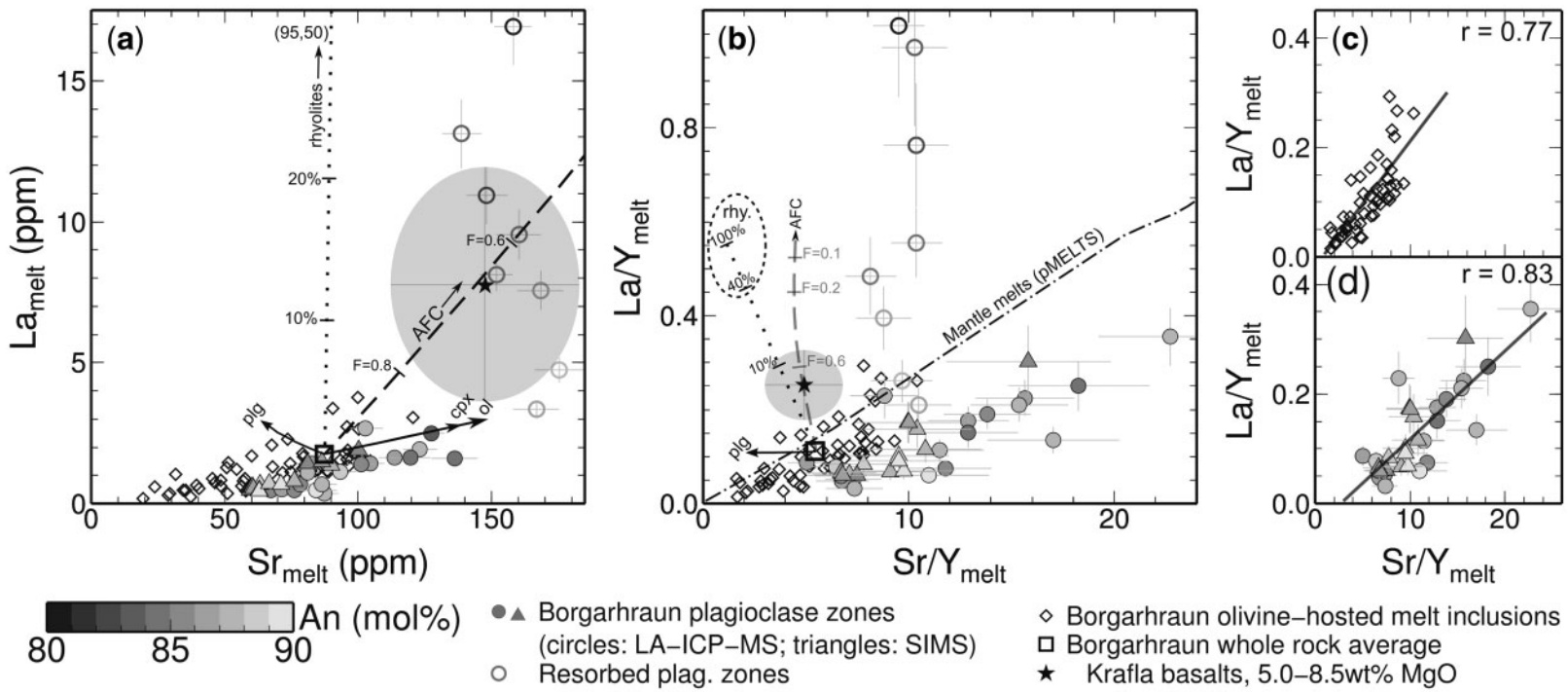

Fig. 8. (a) La vs Sr showing the compositions of melts calculated to be in equilibrium with Borgarhraun plagioclase (open circles are resorbed cores; filled circles are all other zones, shaded by anorthite content). Error bars show 2σ ranges. The black open square shows the mean of Borgarhraun whole-rock samples (Elliott *et al.*, 1991*l*; Hémond *et al.*, 1993; Slater, 1996; Maclennan *et al.*, 2003*b*). Olivine-hosted melt inclusions of Slater (1996) and Maclennan *et al.* (2003*a*) are plotted as open diamonds. Continuous black lines show the effect of 40% fractional crystallization of olivine (ol), clinopyroxene (cpx) and plagioclase (plg) on the average Borgarhraun whole-rock composition, using average partition coefficients for Borgarhraun plagioclase from this study, for Borgarhraun clinopyroxene from Winpenny & Maclennan (2011), and for olivine from McKenzie & O'Nions (1991) (for La and Sr) and Nielsen *et al.* (1992) (for Y). The ±2σ range of compositions of 78 Krafla basalts with $5{\cdot}0 \leq MgO \leq 8{\cdot}5$ wt % is indicated by the grey ellipse; the black star denotes the mean composition. The dotted line shows mixing between the average Borgarhraun whole-rock compositions and an assimilant composition representing Krafla rhyolites (Jónasson, 1994), with 95 ppm Sr, 50 ppm La and 90 ppm Y; the line is labelled with the percentage of assimilant in the total melt. The dashed line indicates AFC following the preferred model of Eiler *et al.* (2000*a*), involving a 1:4 ratio of assimilated to fractionated mass, a ratio of 1:5:5 for ol:plg:cpx crystallization, and an Icelandic andesite composition as the assimilant with 150 ppm Sr, 30 ppm La and 55 ppm Y (data from Nicholson *et al.*, 1991*l*). The AFC line is labelled with the fraction of total liquid mass remaining as compared with the initial mass of liquid. (b) La/Y vs Sr/Y showing the compositions of Borgarhraun plagioclase equilibrium melts; symbols, lines and the data sources as for (a). The dotted ellipse indicates the approximate range of Krafla rhyolite compositions from Jónasson (1994). The dot–dash line labelled 'Mantle melts' shows the La/Y and Sr/Y ratios of instantaneous fractional mantle melts produced by adiabatic decompression melting of uniform peridotitic (i.e. simplified) mantle in the pMELTS program (Ghiorso *et al.*, 2002), using the mantle composition of Workman & Hart (2005), and assuming a mantle potential temperature of 1480°C under northern Iceland (Maclennan *et al.*, 2001*a*) with melts calculated every 1 kbar up an adiabat from 40 kbar to 10 kbar. The effect of 40% plagioclase crystallization is indicated by the fine black line. (c) Linear regression through the olivine-hosted melt inclusion La/Y and Sr/Y data. (d) Linear regression through the plagioclase equilibrium melt La/Y and Sr/Y data (excluding resorbed cores).

correlations observed in the plagioclase equilibrium melt data in Fig. 8a and b, correlations that are critical to this analysis.

Although many different potential assimilants are present in the Icelandic crust, any AFC mechanisms that involve the assimilation of rhyolitic partial melts of altered basalt or Icelandic andesite compositions [the latter favoured by the models of Eiler *et al.* (2000*a*)], would increase La/Y while decreasing Sr/Y, as these melts have lower or equal Sr concentrations compared with average Borgarhraun melts. Lines illustrating these potential assimilation mechanisms are plotted in Fig. 8a and b (see caption for details). These model lines do not reproduce the positive correlation seen between La/Y and Sr/Y of the melts in equilibrium with plagioclase.

Bulk assimilation of existing Icelandic crustal basalts by primitive melts may also occur (e.g. Bindeman *et al.*, 2008); this mechanism has previously been considered for Borgarhraun melts (Eiler *et al.*, 2000*a*; Maclennan *et al.*, 2003*a*). A wide range of crustal basalt compositions is available for assimilation, the trace element compositions of which can vary because of crystal fractionation, mantle melt compositional variability and/or crustal processes. In Fig. 8a and b, the $\pm 2\sigma$ range of 78 whole-rock analyses of basalts from the Krafla volcanic system (adjacent to Theistareykir, and generally displaying more enriched whole-rock compositions) with 5·0–8·5 wt % MgO is shown as a grey field (data from Nicholson *et al.*, 1991; Nicholson & Latin, 1992; Hémond *et al.*, 1993; Maclennan *et al.*, 2001*b*; Stracke *et al.*, 2003*b*; Jónasson, 2005; Kokfelt *et al.*, 2006; Maclennan, 2008*a*; Koornneef *et al.*, 2012). The mean whole-rock composition is shown by a star symbol in each plot. From Fig. 8b it is clear that even if assimilation mechanisms were selective enough to add only high-Sr/Y crustal basalts from this range to the Borgarhraun melt compositions, the observed trends in the Borgarhraun olivine melt inclusions and melts in equilibrium with plagioclase zones could not be reproduced [it should be noted that the trace element compositions of such high-Sr/Y, high-La/Y basalts are themselves likely to reflect mantle melt compositional variability, as Maclennan *et al.* (2003*a*) noted for the case of assimilating a basalt composition similar to that of the Gaesafjoll table mountain (Fig. 1; Maclennan *et al.*, 2002)]. Selective addition of such basalts is also unlikely given the diversity of potential basaltic assimilants in the crust, and it is more likely that assimilation of a range of basalt compositions would occur, either destroying the relationship observed between La/Y and Sr/Y in the Borgarhraun samples, or creating a correlation between these two indices extending from Borgarhraun melt compositions to an average crustal basalt composition for northern Iceland (most probably less enriched than the average of the Krafla basalts shown in Fig. 8b); neither of these scenarios is evident from the plotted data. It should be noted also that large amounts of assimilation of crustal basalts, many of which are likely to be more evolved than Borgarhraun melts, would also affect Borgarhraun whole-rock major element compositions, an effect that is not observed (Maclennan *et al.*, 2003*a*, 2003*b*). Even if assimilation of basalts could explain the trace element systematics of the Borgarhraun crystal and melt inclusion data, very large amounts of bulk addition of the average basalt assimilant to the most depleted Borgarhraun melts would be required (~60% by mass) to reproduce the highest La/Y concentrations observed in Borgarhraun olivine-hosted melt inclusions. Although assimilation models for up to ~50% bulk addition of crustal rocks have been proposed (Bindeman *et al.*, 2008), assimilation of this magnitude would be likely to decrease the temperature of Borgarhraun melts to the point of inconsistency with the temperatures of crystallization indicated by Borgarhraun whole-rock compositions (Maclennan *et al.*, 2003*a*) and of clinopyroxene formed throughout the crystallization of Borgarhraun melts [$1260 \pm 14^{\circ}$C (1σ); Winpenny & Maclennan, 2011].

The positive correlations for the Borgarhraun data therefore best fit with the hypothesis that, like olivine-hosted melt inclusions, the trace element compositions of melts in equilibrium with plagioclase reflect primary mantle melt compositional variability. A range of illustrative fractional mantle melt compositions calculated using pMELTS (Ghiorso & Sack, 1995; Wood & Blundy, 1997; Ghiorso *et al.*, 2002; Smith & Asimow, 2005) is shown in Fig. 8b, displaying a positive correlation between La/Y and Sr/Y consistent with the trends observed in the equilibrium melt data.

δ^{18}O VARIABILITY IN BORGARHRAUN PLAGIOCLASE

The δ^{18}O range of all Borgarhraun plagioclase zones is +4·02–5·87‰. Excluding the resorbed cores, the range is +4·45–5·87‰. The range in resorbed cores is more limited, at +4·06–5·02‰. The previously described textural and trace element observations indicate that the resorbed cores form a group distinct from the rest of the plagioclase zones (seemingly showing evidence for crustal processes involving an evolved and/or crustally contaminated basaltic melt, as mentioned in the previous section), so they are left aside during the following discussion. As significant CaAl–NaSi diffusion was observed to have occurred in these cores, it is conceivable that they inherited their trace element concentrations and $^{18}O/^{16}O$ ratios by diffusion from an evolved melt in which they were being held, prior to crystallization of the other zones from primitive melts (note that the compositions of these other zones show no sign of being affected by the evolved melt); a crustal origin for low δ^{18}O cannot therefore be ruled out for

these cores. The main focus of this section, however, is the remaining majority of the plagioclase zones, that were also the focus of previous sections.

The $\delta^{18}O$ values of plagioclase zones, excluding the resorbed cores, are shown in Fig. 9. The values plotted are for melts in equilibrium with the crystal phases, $\delta^{18}O_{melt}$, assuming a constant plagioclase–melt isotope fractionation ($\Delta^{18}O_{plag-melt}$) of 0·2‰. This value is based on the work of Chiba *et al.* (1989), who gave an anorthite–forsterite fractionation of 0·71‰ at 1260°C, and follows the work of Eiler *et al.* (1997, 2000*a*) and Thirlwall *et al.* (2006) in using a melt–forsteritic olivine fractionation of 0·5‰. It is also similar to values determined from coexisting natural glass and plagioclase (e.g. Macpherson & Mattey, 1998). The melt-equivalent oxygen isotope ratios of crystal phases, calculated using these fractionation data, are denoted by $\delta^{18}O_{melt}$.

Figure 9a shows that $\delta^{18}O$ variability of ~1·4‰ (much greater than the propagated precision, typically 0·3–0·4‰, 2σ) is present in $\sim An_{84-90}$ plagioclase zones. These oxygen isotope data show good correlations with La/Y (Fig. 9b, $r = -0·76$) and Sr/Y (Fig. 9c, $r = -0·68$) in the plagioclase equilibrium melts, with $\delta^{18}O_{melt}$ decreasing as La/Y and Sr/Y increase. Because the positive correlation between the Sr/Y and La/Y ratios of the equilibrium melts (Fig. 8b) was shown above to result from the variability in trace element compositions of mantle melts, the negative correlations of the same La/Y and Sr/Y data with $\delta^{18}O$ of the plagioclase zones strongly indicate that variability in $\delta^{18}O$ in the plagioclase zones arises from oxygen isotope variability in mantle melts.

To illustrate further that crustal processes are not the likely cause of the correlations in Fig. 9b and c, various model curves are plotted showing the effects of AFC and mixing with rhyolitic or basaltic assimilants. Although the model curves are roughly consistent with the trend in Fig. 9b of increasing La/Y with decreasing $\delta^{18}O_{melt}$, they cannot explain the correlation seen in Fig. 9c, the Sr/Y versus $\delta^{18}O_{melt}$ plot. Assuming a lower $\delta^{18}O$ for the basaltic assimilant would not improve the fit of the model to the data.

The correlations of $\delta^{18}O$ with trace element ratios therefore strongly support the suggestions of Maclennan *et al.* (2003*a*) that a low-$\delta^{18}O$ signature exists in some of the mantle melts that mix in the Icelandic lower crust, and thus that low-$\delta^{18}O$ material is present in the mantle itself under Iceland. Enriched (high-La/Y and -Sr/Y) melts, sourced from the garnet stability field, appear to have $\delta^{18}O$ lower than the typical MORB range (+5·21–5·81‰). The lowest $\delta^{18}O_{melt}$ value attributable to a mantle melt composition is +4·3‰, giving an olivine-equivalent value ($\delta^{18}O_{ol}$) of ~+3·8‰. Given the accuracy of the plagioclase $\delta^{18}O$ data (estimated at ±0·4‰ for the dataset as a whole), combined with the likely precision of mineral–melt and mineral–mineral oxygen isotope fractionations (~0·1–0·2‰), the propagated accuracy estimate for these lowest olivine- and melt-equivalent $\delta^{18}O$ values is ±0·5‰. It should be noted, however, that the calculated $\delta^{18}O_{melt}$ values for the plagioclase zones that have the most depleted (MORB-like) equilibrium melt compositions are ~5·5‰, the same as for average MORB, which may suggest that the accuracy is perhaps better than 0·5‰.

DISCUSSION

Trace element variability across most Borgarhraun plagioclase zones has been interpreted as reflecting the compositional diversity of mantle melts, prior to or during mixing of these melts in the lower Icelandic crust, the same interpretation as for the variability in trace element compositions of Borgarhraun olivine-hosted melt inclusions (Maclennan *et al.*, 2003*a*) and clinopyroxene compositional zones (Winpenny & Maclennan, 2011). The three resorbed cores may preserve evidence for crustal processes such as melt mixing or assimilation of pre-existing crustal lithologies. Excluding the resorbed cores, plagioclase $\delta^{18}O$ variability is interpreted to reflect heterogeneity in $\delta^{18}O$ of the Icelandic mantle source. Some aspects of the data will now be explored further, and the origin of low $\delta^{18}O$ in the Icelandic mantle and associated mass-balance issues will be considered.

A limited role for diffusion in Borgarhraun plagioclase

The existence of trace element and $\delta^{18}O$ variability in single Borgarhraun plagioclase crystals indicates that diffusion during crustal storage has not removed the variability in these indices amongst crystal zones. In addition, significant diffusion across zones would act to destroy the correlations shown in Figs 8 and 9, as it would decouple $\delta^{18}O$ and the concentration of Sr from those of La and Y, which diffuse more slowly.

The robustness of the correlations of $\delta^{18}O_{melt}$ with La/Y and Sr/Y, and the fact that these are highly unlikely to occur by chance, can be illustrated by observing the range of correlation coefficients (r) and associated p values (the probability that a random, uncorrelated distribution would produce a better r value than that from the observed distribution) calculated from a set of simulated fits to the correlations. In these simulations, values for La/Y and $\delta^{18}O$, or Sr/Y and $\delta^{18}O$, were drawn at random from Gaussian distributions centred on each datum point in Fig. 9, using the errors listed in Supplementary Data Electronic Appendix 1 as standard deviations for the distributions. This method produced a different line of fit, and thus different r and p values, for each simulation. The test statistic for the p values follows a t-distribution. In 95% of the simulations, $|r|$ values were ≥0·64 for the La/Y–$\delta^{18}O$ correlation and ≥0·57 for the Sr/Y–$\delta^{18}O$ correlation.

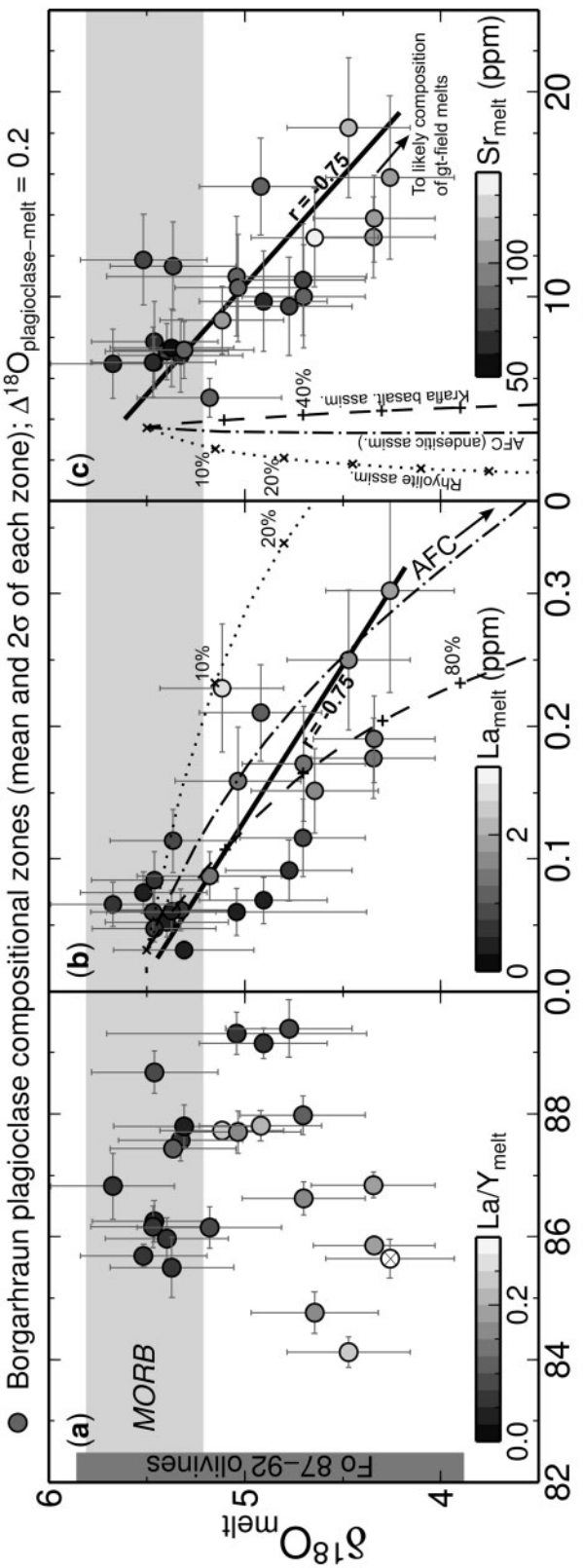

Fig. 9. Oxygen isotope data from Borgarhraun plagioclase zones (excluding resorbed cores), expressed as $\delta^{18}O_{melt}$, using a plagioclase–melt fractionation of 0·2‰, plotted against (a) anorthite content of the compositional zones, (b) La/Y of the melt calculated to be in equilibrium with the plagioclase zones, and (c) Sr/Y of the equilibrium melt. The grey field in each plot shows the range of $\delta^{18}O$ of MORB (Thirlwall *et al.*, 2006). The range of $\delta^{18}O_{melt}$ of olivine crystals from Borgarhraun (Maclennan *et al.*, 2003*b*) is shown as a dark grey bar along the *y*-axis in (a). The datum point in (a) with an internal cross does not have trace element data. Continuous lines in (b) and (c) are linear regressions through the data. Dotted lines show mixing of a putative depleted melt composition (50 ppm Sr, 0·45 ppm La, 14·2 ppm Y, $\delta^{18}O = +5.5‰$) with a typical Icelandic rhyolite composition as in Fig. 8, which has a $\delta^{18}O$ value of +2‰ [following Nicholson *et al.* (1991) and Eiler *et al.* (2000*a*)]. Dot–dash lines show AFC with the same mechanism as described for Fig. 8, but starting with the putative depleted melt composition; the assimilant has a $\delta^{18}O$ value of 0‰ (Eiler *et al.*, 2000*a*). The dashed lines illustrate bulk addition to the putative depleted melt composition of an average Krafla basalt composition, as denoted by the black stars in Fig. 8, assuming a $\delta^{18}O$ value of +3·5‰ for the assimilant. '×' symbols on mixing lines show 10% increments of assimilant addition; '+' symbols show 20% increments.

Values of p in 95% of simulations were $<1{\cdot}26 \times 10^{-4}$ and $<1{\cdot}30 \times 10^{-4}$ respectively.

In the worst case, that each crystal effectively represents one independent datum point (as a result of diffusion; a scenario that is, in any case, not supported by the fact that variability in trace elements and $\delta^{18}O$ is observed in some crystals), the correlations from the data still support the conclusion. Using the average $\delta^{18}O$ and trace element compositions in each crystal and their standard errors, $|r|$ values calculated for sets of simulations carried out in the same way as above are $\geq 0{\cdot}57$ in 95% of cases for the La/Y–$\delta^{18}O$ correlation and $\geq 0{\cdot}61$ for the Sr/Y–$\delta^{18}O$ correlation. Similarly, values of p are $<8{\cdot}92 \times 10^{-2}$ and $<1{\cdot}48 \times 10^{-5}$ respectively. Although the former of these two probabilities is distinctly higher than the latter, it should be noted that the Sr/Y–$\delta^{18}O$ correlation is the more important for distinguishing the mantle $\delta^{18}O$ source from crustal mechanisms (Fig. 9c). It is therefore possible to establish that diffusional re-equilibration of crystals during crustal storage has not exerted an important influence upon the observed correlations and interpretations.

Evidence for mantle $\delta^{18}O$ from three crystal phases from Borgarhraun

It is striking that $\delta^{18}O$ data from whole olivine and clinopyroxene crystals from Borgarhraun and from most of the plagioclase compositional zones are all consistent with a mantle origin for oxygen isotope variability. The $\delta^{18}O$ data of Maclennan *et al.* (2003*a*) show variability of >1‰ between Fo_{90} olivines, and enriched melt inclusions (La/Yb > 2) are held in olivines with $\delta^{18}O_{melt}$ of ~+4‰, whereas depleted inclusions (La/Yb <0·5) typically have host olivines with $\delta^{18}O_{melt}$ of ~+5·5‰. The clinopyroxene $\delta^{18}O$ data (+4·6–5·4‰) of Maclennan *et al.* (2003*a*) show a negative correlation with crystal La/Yb ratios and a positive correlation with crystal Mg# over the range Mg# 87–91 ($r = -0{\cdot}79$ and +0·79 respectively). These correlations are in contrast to the spread of $\delta^{18}O$ variability in olivine at high forsterite contents, and can be rationalized if low $\delta^{18}O$ originates in the mantle. The explanation is based on the conclusion of Winpenny & Maclennan (2011) that high-Mg# clinopyroxenes are crystallized only from depleted (low LREE/HREE) mantle melts whereas ~Fo_{90} olivine can be formed from all mantle melt compositions. If the depleted mantle melts have $\delta^{18}O_{melt} = +5{\cdot}5$‰ and enriched mantle melts have lower $\delta^{18}O$ values, then fractional crystallization with simultaneous mixing of depleted (clinopyroxene-saturated) melts with enriched (initially cpx-undersaturated) melts would cause clinopyroxene LREE/HREE ratios to increase slightly while $\delta^{18}O$ and Mg# of clinopyroxene drop, thereby explaining the correlations seen in the clinopyroxene data of Maclennan *et al.* (2003*a*). The ability of mantle $\delta^{18}O$ heterogeneity to explain the differing trace element and $\delta^{18}O$ systematics of three Borgarhraun crystal phases (olivine, clinopyroxene and plagioclase) provides a strong argument for its validity as the cause of $\delta^{18}O$ heterogeneity.

Length scale of mantle $\delta^{18}O$ heterogeneity

The existence of variability in $\delta^{18}O$ attributable to mantle heterogeneity in samples from a single volcanic system, Theistareykir, further implies that the Icelandic mantle is heterogeneous in $\delta^{18}O$ on a length scale smaller than the width of the melting region underneath the system. This width is <100 km, based on compositional dichotomies and Sr–Nd–Pb isotope ratio variability between pairs of volcanoes separated by tens of kilometres (e.g. Thirlwall *et al.*, 2004; Sinton *et al.*, 2005; Sims *et al.*, 2013) and seismological studies (Du & Foulger, 2004). Like the oxygen isotope variability preserved in plagioclase from the Borgarhraun flow, high-amplitude variability in Pb isotope ratios within single Icelandic lava flows (and even in single hand specimens) has been shown to exist through analyses of melt inclusions (Maclennan, 2008*b*). Sr isotope ratios from plagioclase crystals in single flows can also show significant diversity (Halldorsson *et al.*, 2008), which is also indicative of short length scale isotopic heterogeneity in the Icelandic mantle.

The association of low $\delta^{18}O$ with high La/Y and Sr/Y of the melts in equilibrium with plagioclase zones suggests that the low-$\delta^{18}O$ signature is associated with enriched melts produced in the garnet stability field of the mantle. Well-defined correlations between indices of trace element enrichment and isotope systematics (e.g. Sr, Nd, Pb, Hf, Os isotopes) in basalts (including Theistareykir basalts; Stracke *et al.*, 2003*a*) and melt inclusions (Maclennan, 2008*b*) have been used in the past to support the hypothesis that some material in the Icelandic mantle source, isotopically distinct from depleted peridotite, has a lower solidus temperature than the ambient mantle and melts extensively in the stability field of garnet (e.g. Hirschmann & Stolper, 1996; Sims *et al.*, 2013). The melts produced have distinct isotopic and trace element signatures, including high LREE/HREE and high LREE/Y. The low-$\delta^{18}O$ signature is therefore likely to be associated with the same, isotopically distinct material. This association was proposed by Thirlwall *et al.* (2006), on the basis of correlations of olivine $\delta^{18}O$ with Sr, Nd and Pb isotope ratios of whole-rock samples from SW Iceland and the Reykjanes Ridge. Furthermore, because indices of trace element enrichment correlate with the major element compositions of basalts, and major element compositions are controlled to a large degree by source mineralogy (Shorttle & Maclennan, 2011), it is likely that the fusible material hosting the low-$\delta^{18}O$ signature has a mineralogy distinct from that of the ambient Icelandic mantle.

A lower bound of ~10 m on the length scale of domains hosting isotopic heterogeneities in the Icelandic mantle has been suggested from the models of Kogiso *et al.* (2004),

which consider the preservation of Os isotope signatures in pyroxenite bodies of varying dimensions hosted in peridotite mantle over 10^9 years. Unfortunately, given that oxygen diffusion is less rapid than Os diffusion in the silicate phases of peridotite or pyroxenite at mantle temperatures (Farver, 2010), no additional constraint on the minimum length scale of heterogeneities is offered by the current dataset. Nevertheless, the conclusion that short length scale (<100 km), high-amplitude (~1‰) variability in $\delta^{18}O$ exists in the mantle beneath Iceland, and can be resolved through analyses of a single basalt flow, has not previously been demonstrated.

Possible mantle sources for Borgarhraun plagioclase $\delta^{18}O$ heterogeneity

The range in $\delta^{18}O_{melt}$ for MORB is small (+5·21–5·81‰; as noted by Thirlwall *et al.*, 2006). A $\delta^{18}O_{melt}$ value of ~+4·3‰ for Borgarhraun plagioclase, attributable to the Icelandic mantle, therefore represents a significant departure from the normal MORB range.

Subducted, recycled oceanic crust has been favoured by a number of researchers as a candidate for the enriched, fusible material that melts in the stability field of garnet under Iceland (e.g. Hofmann & White, 1982; Saunders *et al.*, 1988; Weaver, 1991; Chauvel & Hémond, 2000; Breddam, 2002; Macpherson *et al.*, 2005; Kokfelt *et al.*, 2006). Some workers have further argued that part of the isotopic diversity of Icelandic basalts has its origins in materials other than recycled MORB (e.g. Stracke *et al.*, 2003*a*; Thirlwall *et al.*, 2004, 2006); for instance, recycled ocean island basalt (McKenzie *et al.*, 2004). Sobolev *et al.* (2007) argued that recycled oceanic crust, initially present as eclogite in the mantle, produces silica-rich melts that react with the enclosing peridotite, converting it to olivine-free pyroxenite. After reaction, this pyroxenite would be isotopically distinct from the surrounding peridotite and would in turn melt to produce the enriched mantle melt compositions observed in primitive Icelandic basalts and melt inclusions. The suite of Icelandic basalts studied by Sobolev *et al.* (2008) indicated that the proportion of erupted melt ultimately derived from recycled material may be in the region of 20% for some enriched Icelandic compositions, on the basis that pyroxenite is formed through a reaction of eclogite-derived melt and peridotite in roughly equal proportions by mass. Another constraint on the contribution of recycled material to melt generation under Iceland was noted by Maclennan *et al.* (2003*a*): major element compositions of melts of peridotite–basalt mixture KG-2 (Kogiso *et al.*, 1998) closely resemble those of enriched Icelandic basalts. KG-2 is composed of peridotite KLB-1 and average MORB in a 2:1 ratio, the latter composition probably being equivalent to recycled crustal material. This resemblance was further investigated across a large range of Icelandic basalt compositions by Shorttle & Maclennan (2011), who concluded that a source similar to KG-2 or KG-1 (a 1:1 MORB–KLB-1 mix; Kogiso *et al.*, 1998) with ~40% recycled MORB material could produce the most enriched Icelandic basalt compositions. A source similar to KG-1 or KG-2 for the most enriched Icelandic basalts would therefore indicate that the proportion of these basalts ultimately derived from recycled material is around 40%.

Thirlwall *et al.* (2006) gave consideration to the type of recycled material that may form low-$\delta^{18}O$ heterogeneities in the mantle, and noted that alteration of the upper oceanic crust at <400°C by seawater with $\delta^{18}O = \sim 0‰$ results in elevated crustal $\delta^{18}O$ values (≳5·5‰). Higher temperature alteration of lower crustal gabbros, on the other hand, causes $\delta^{18}O$ to decrease. Measured values of altered gabbro may be as low as +1·7‰ (Stakes & Taylor, 1992), but mean gabbro values from various studies of ophiolites and drill cores are all ≥+4·0‰. The $\delta^{18}O$ profile of oceanic crust is thought to be unchanged by dehydration processes during subduction (Valley, 1986; Miller *et al.*, 2001). The $\delta^{18}O$ of Archaean and early Palaeozoic seawater may have had a much lighter oxygen isotopic composition compared with seawater today (e.g. Azmy *et al.*, 1998; Veizer *et al.*, 1999; Jaffrés *et al.*, 2007; Joachimski *et al.*, 2009), but ancient ophiolites have $\delta^{18}O$ profiles indistinguishable from more modern analogues and drill cores of present-day oceanic crust (Hoffman *et al.*, 1986; Lécuyer & Fourcade, 1991; Holmden & Muehlenbachs, 1993; Muehlenbachs *et al.*, 2003; Furnes *et al.*, 2007).

To satisfy the constraint that the contribution of melt derived from recycled crustal material to enriched Icelandic basalt compositions is no more than ~40%, then in the case that these enriched basalts have the lowest $\delta^{18}O_{melt}$ value attributed to a mantle origin in this study (+4·3 ± 0·5‰), the recycled material in the mantle source must have a $\delta^{18}O$ value in the range of ~+1·3–3·7‰ (assuming an ambient mantle $\delta^{18}O$ of ~5·5‰). The case that the most enriched Icelandic basalts have $\delta^{18}O$ of ~4·3‰ is perhaps reasonable, as the highest La/Y ratios of melts in equilibrium with the Borgarhraun plagioclase appear to be roughly similar to the ratio for the enriched basaltic endmember of Shorttle & Maclennan (2011), at 0·355 and 0·329 respectively (the depleted endmember has a La/Y of 0·081). The required $\delta^{18}O$ range of ~+1·3–3·7‰, however, is lower than the mean values of gabbros observed in ophiolites and drill cores (≥+4‰; Thirlwall *et al.*, 2006) and so recycling of gabbroic material alone under Theistareykir can explain the range of $\delta^{18}O$ in Borgarhraun plagioclase only if its $\delta^{18}O$ is below these mean values. It should be noted that a core–mantle boundary origin for the low-$\delta^{18}O$ signature and an origin by recycling of high-latitude, low-$\delta^{18}O$, thick oceanic crust similar to that of Iceland have been ruled out by Macpherson *et al.* (2005) and Thirlwall *et al.* (2006), respectively. This is because there is no clear

influence from core material on siderophile element concentrations in Icelandic basalts, and recycling of a thick, buoyant crustal body similar to Iceland was considered unlikely.

It is possible that a small part of the ~1·4‰ range in the Borgarhraun plagioclase crystals that reflect mantle melt $\delta^{18}O$ values is caused by melting of different lithologies in the mantle. For instance, using the mineral–mineral isotope fractionation factors outlined by Eiler (2001) and a melt–olivine fractionation of 0·4‰, an enriched melt of an olivine-free garnet pyroxenite source could, solely as a result of its mineralogy, be ~0·3‰ lighter than a melt of the lherzolite source of depleted melts. Uncertainties in source mineralogy and fractionation factors (particularly for crystal–melt fractionation) make this effect difficult to quantify reliably, but it could lessen the $\delta^{18}O$ variability required in the Icelandic mantle source by the plagioclase data to ~1‰.

Apart from gabbros in ophiolites and drill cores with mean $\delta^{18}O$ values of ≥+4·0‰, eclogite xenoliths found in kimberlites are widely accepted to be fragments of ancient, subducted oceanic crust, and are diverse in $\delta^{18}O$, from +2·4 to ~+8‰ (Garlick *et al.*, 1971; MacGregor & Manton, 1986; Ongley *et al.*, 1987; Schulze *et al.*, 2000; Shirey *et al.*, 2001; Jacob, 2004; Jacob *et al.*, 2005). It has recently been suggested that Type II eclogites from the Roberts Victor mine retain original (post-subduction) $\delta^{18}O$ in the range of ~2–4·5‰ (mean ~3·5‰), whereas the more abundant Type I eclogites carry the imprint of a later metasomatic process that strongly modified their major-element and trace-element compositions and shifted their $\delta^{18}O$ to higher values (mean ~6·5‰; Gréau *et al.*, 2011). Therefore recycled oceanic crustal material in the Icelandic mantle source with the $\delta^{18}O$ composition of many Type II eclogites could explain the $\delta^{18}O$ range of Borgahraun plagioclase, but its origins are uncertain.

Although it is perhaps still unclear whether recycled, lower oceanic crustal gabbros alone could be the source of the low-$\delta^{18}O$ signature in primitive Icelandic basalts, this does not preclude a role for similar recycled material in the formation of isotopic variability in the basalts, especially as more than one enriched mantle endmember may be involved in the melting beneath Iceland (Chauvel & Hémond, 2000; Stracke *et al.*, 2003*a*; Thirlwall *et al.*, 2004; Kokfelt *et al.*, 2006). Crustal recycling is indeed possible in other locations globally: for instance, recycled, high-$\delta^{18}O$ upper oceanic crust has been invoked by Eiler *et al.* (2000*b*) to explain $\delta^{18}O$ systematics in basalts from the East Pacific Rise, Mid-Atlantic Ridge and Indian Ocean, and by Eiler *et al.* (1996) for high $\delta^{18}O$ values in Hawaiian olivines. Further studies of oxygen isotopes in primitive Icelandic basalts and their macrocrysts need to be made to fully constrain the $\delta^{18}O$ range of the mantle beneath Iceland, and estimates of the proportion of melt derived from recycled material need to be better constrained before models of recycling of low-$\delta^{18}O$ material are carried any further.

McKenzie *et al.* (2004) suggested that the isotopic signature of the enriched material under Theistareykir may be inherited from recycling of a basaltic ocean island that has been altered by interaction with low-$\delta^{18}O$ water. This mechanism is appealing for matching the compositional variation observed within the Borgarhraun eruption, or perhaps on the scale of a single volcanic system such as Theistareykir. Because large volumes of low-$\delta^{18}O$ material are required in the source regions to influence the mean oxygen isotopic composition of the melt, it is not clear that recycling of ocean islands would be expected to provide a widespread regional signature in $\delta^{18}O$, evidence for which comes from a number of previous studies suggesting that low $\delta^{18}O$ observed in samples from across Iceland and the Reykjanes Ridge also reflects mantle heterogeneity (Macpherson *et al.*, 2005; Thirlwall *et al.*, 2006). However, because previous studies did not use microanalysis to directly link the $\delta^{18}O$ variations to trace element compositions, the elemental and radiogenic isotopic signature of the low-$\delta^{18}O$ material is not as well constrained under central Iceland or the Reykjanes Ridge as it is under Theistareykir. To test the suitability of recycled ocean islands as the host of the low-$\delta^{18}O$ signature in the North Atlantic, it will be necessary to make focused microanalytical studies of isotopic and trace element variation in a number of locations across the region.

Although low $\delta^{18}O$ in other ocean island groups such as the Canary Islands and Azores has been interpreted by some researchers in terms of melting of a mantle containing recycled oceanic crust and mantle lithosphere (Turner *et al.*, 2007; Day *et al.*, 2009, 2010; Gurenko *et al.*, 2011), the unusually low $\delta^{18}O$ that this study has isolated and attributed to the enriched mantle source regions of basalts in Iceland and its surrounding ridges may require the involvement of recycled material with lower $\delta^{18}O$ than previously considered for other island groups (Fig. 10). The current difficulty in explaining the origin of the recycled material highlights the need for further investigation to resolve the relationship between basalt composition and the nature of recycled materials in their mantle source regions.

CONCLUSIONS

The main findings from major element, trace element and oxygen isotope analyses of Borgarhraun plagioclase zones can be summarized as follows.

(1) Trace element systematics of the melts calculated to be in equilibrium with many of the Borgarhraun plagioclase zones indicate that variability in trace element ratios (La/Y, Sr/Y) arises from the diversity of primary mantle melt compositions. This record of

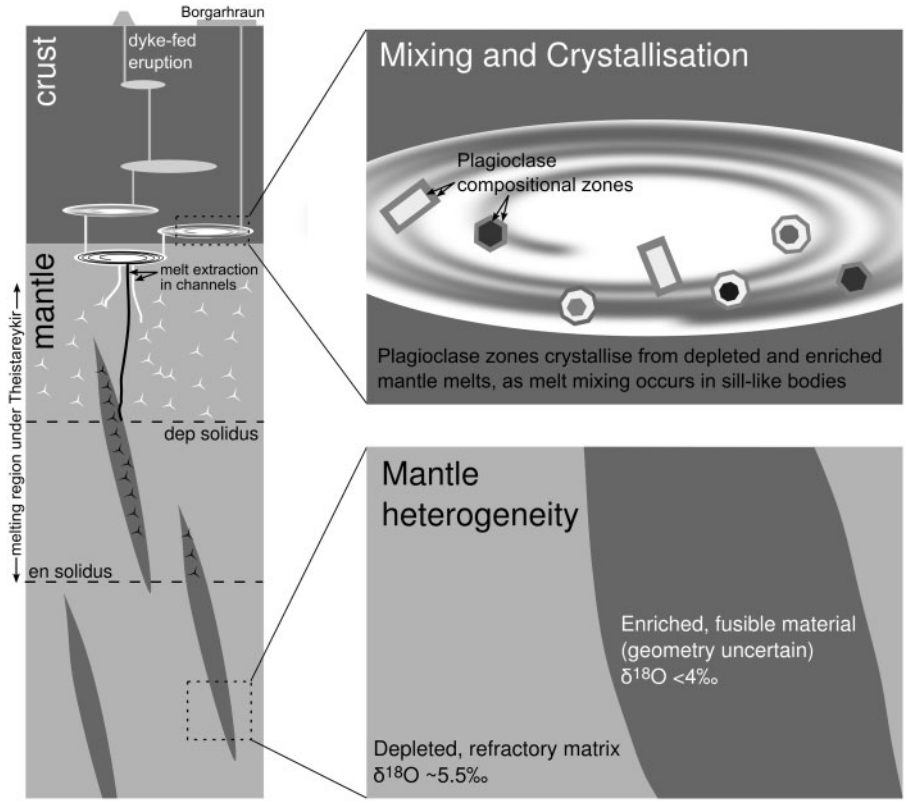

Fig. 10. Schematic illustration of the processes involved in the production of the record of compositional and isotopic heterogeneity of mantle melts preserved in Borgarhraun plagioclase compositional zones. The processes are melting of heterogeneous mantle (within a plume setting), melt extraction to near-Moho magma chambers in channels, and subsequent growth of crystals from the melts in these magma chambers during or after the onset of crystallization of primitive crystal phases, including anorthitic plagioclase. Melt production from fusible, enriched material in the mantle (dark grey ellipses) and depleted, refractory mantle is represented by black and white tri-stars, beginning at the enriched (en) or depleted (dep) solidus, respectively. It should be noted that the geometry and dimensions of the enriched heterogeneities in the mantle, the channels and sills are poorly known. The enriched heterogeneities in the mantle are the source of low-$\delta^{18}O$ melts. The source lithology and the process of fractional melting of depleted mantle over the depth range of the melting column contribute to trace element heterogeneity of the melts that enter mantle channels and near-Moho sills.

mantle melt compositions is similar to that observed in the melts calculated to be in equilibrium with Borgarhraun clinopyroxene (Winpenny & Maclennan, 2011), and olivine-hosted melt inclusions (Maclennan *et al.*, 2003*a*).

(2) Correlations between $\delta^{18}O$ of plagioclase zones and La/Y and Sr/Y ratios of plagioclase equilibrium melts cannot be adequately explained by crustal processes. The most likely explanation is that enriched melts from the garnet stability field of the Icelandic mantle, which have high La/Y and Sr/Y ratios, have a low-$\delta^{18}O$ signature. This signature stems from the presence of readily fusible material in the Icelandic mantle with $\delta^{18}O$ lower than the ambient mantle value of ~5·5‰.

(3) The existence of a range in $\delta^{18}O$ of ≥1‰ attributable to a mantle source in a single Icelandic basalt flow indicates heterogeneity in $\delta^{18}O$ in the Icelandic mantle over a length scale of <100 km.

(4) The lowest $\delta^{18}O$ value of plagioclase that can be ascribed to a mantle origin in this study is $+4{\cdot}5 \pm 0{\cdot}4$‰, which gives melt- and olivine-equivalent values of $+4{\cdot}3 \pm 0{\cdot}5$‰ and $+3{\cdot}8 \pm 0{\cdot}5$‰, respectively. The reason for the low-$\delta^{18}O$ signature in the mantle is unclear, but the signature may result from the recycling of a crustal lithology that experienced high-temperature hydrothermal alteration.

ACKNOWLEDGEMENTS

Thanks are due to the staff of the NERC Ion Microprobe Facility, in particular John Craven for assistance with oxygen isotope analyses. Jason Day, Martin Walker, Andy Buckley and Chiara Petrone gave valuable analytical assistance, and Mike Bickle provided additional guidance. Useful discussions were had with Marie Edmonds and Colin Macpherson, who both examined the PhD thesis of

B.W., of which this work forms a part. Useful and perceptive reviews were provided by John Eiler, James Day and Colin Macpherson.

FUNDING

This work was supported by a Natural Environment Research Council studentship to B.W. (NE/F007183/1), a Natural Environment Research Council young investigator grant to J.M. (NE/E001254/1) and a Natural Environment Research Council Ion Microprobe Facility award (IMF 365/1008).

SUPPLEMENTARY DATA

Supplementary data for this paper are available at *Journal of Petrology* online.

REFERENCES

Albarède, F. & Bottinga, Y. (1972). Kinetic disequilibrium in trace element partitioning between phenocrysts and host lava. *Geochimica et Cosmochimica Acta* **36**, 141–156.

Azmy, K., Veizer, J., Bassett, M. G. & Copper, P. (1998). Oxygen and carbon isotopic composition of Silurian brachiopods: implications for coeval seawater and glaciations. *Geological Society of America Bulletin* **110**, 1499–1512.

Beattie, P. (1993). Olivine–melt and orthopyroxene–melt equilibria. *Contributions to Mineralogy and Petrology* **115**, 103–111.

Bédard, J. H. (2006). Trace element partitioning in plagioclase feldspar. *Geochimica et Cosmochimica Acta* **70**, 3717–3742.

Bender, J. F., Hodges, F. N. & Bence, A. E. (1978). Petrogenesis of basalts from the project FAMOUS area: experimental study from 0 to 15 kbars. *Earth and Planetary Science Letters* **41**, 277–302.

Bindeman, I., Gurenko, A., Sigmarsson, O. & Chaussidon, M. (2008). Oxygen isotope heterogeneity and disequilibria of olivine crystals in large volume Holocene basalts from Iceland: Evidence for magmatic digestion and erosion of Pleistocene hyaloclastites. *Geochimica et Cosmochimica Acta* **72**, 4397–4420.

Bindeman, I., Gurenko, A., Carley, T., Miller, C., Martin, E. & Sigmarsson, O. (2012). Silicic magma petrogenesis in Iceland by remelting of hydrothermally altered crust based on oxygen isotope diversity and disequilibria between zircon and magma with implications for MORB. *Terra Nova* **24**, 227–232.

Bindeman, I. N., Davis, A. M. & Drake, M. J. (1998). Ion microprobe study of plagioclase–basalt partition experiments at natural concentration levels of trace elements. *Geochimica et Cosmochimica Acta* **62**, 1175–1193.

Bindeman, I. N., Sigmarsson, O. & Eiler, J. (2006). Time constraints on the origin of large volume basalts derived from O-isotope and trace element mineral zoning and U-series disequilibria in the Laki and Grímsvötn volcanic system. *Earth and Planetary Science Letters* **245**, 245–259.

Blundy, J. & Wood, B. (1994). Prediction of crystal–melt partition coefficients from elastic moduli. *Nature* **372**, 452–454.

Breddam, K. (2002). Kistufell: Primitive melt from the Iceland mantle plume. *Journal of Petrology* **43**, 345–373.

Burnard, P. & Harrison, D. (2005). Argon isotope constraints on modification of oxygen isotopes in Iceland basalts by surficial processes. *Chemical Geology* **216**, 143–156.

Carpenter, M. A., McConnell, J. D. C. & Navrotsky, A. (1985). Enthalpies of ordering in the plagioclase feldspar solid solution. *Geochimica et Cosmochimica Acta* **49**, 947–966.

Chauvel, C. & Hémond, C. (2000). Melting of a complete section of recycled oceanic crust: trace element and Pb isotopic evidence from Iceland. *Geochemistry, Geophysics, Geosystems* **1**, 1001, doi:10.1029/1999GC000002.

Cherniak, D. J. (2002). REE diffusion in feldspar. *Chemical Geology* **193**, 25–41.

Cherniak, D. J. (2010). Cation diffusion in feldspars. In: Zhang, Y. & Cherniak, D. J. (eds) *Diffusion in Minerals and Melts. Mineralogical Society of America and Geochemical Society, Reviews in Mineralogy and Geochemistry* **72**, 691–734.

Cherniak, D. J. & Watson, E. B. (1992). A study of strontium diffusion in K-feldspar, Na–K feldspar and anorthite using Rutherford Backscattering Spectroscopy. *Earth and Planetary Science Letters* **113**, 411–425.

Cherniak, D. J. & Watson, E. B. (1994). A study of strontium diffusion in plagioclase using Rutherford backscattering spectroscopy. *Geochimica et Cosmochimica Acta* **58**, 5179–5190.

Chiba, H., Chacko, T., Clayton, R. N. & Goldsmith, J. R. (1989). Oxygen isotope fractionations involving diopside, forsterite, magnetite, and calcite: Application to geothermometry. *Geochimica et Cosmochimica Acta* **53**, 2985–2995.

Condomines, M., Gronvold, K., Hooker, P. J., Muehlenbachs, K., O'Nions, R. K., Oskarsson, N. & Oxburgh, E. R. (1983). Helium, oxygen, strontium and neodymium isotopic relationships in Icelandic volcanics. *Earth and Planetary Science Letters* **66**, 125–136.

Coogan, L. A., Manning, C. E., Wilson, R. N. & E.I.M.F. (2007). Oxygen isotope evidence for short-lived high-temperature fluid flow in the lower oceanic crust at fast-spreading ridges. *Earth and Planetary Science Letters* **260**, 524–536.

Danyushevsky, L. V., Carroll, M. R. & Falloon, T. J. (1997). Origin of high-An plagioclase in Tongan high-Ca boninites; implications for plagioclase–melt equilibria at low $P(H_2O)$. *Canadian Mineralogist* **35**, 313–326.

Danyushevsky, L. V., Perfit, M. R., Eggins, S. M. & Falloon, T. J. (2003). Crustal origin for coupled 'ultra-depleted' and 'plagioclase' signatures in MORB olivine-hosted melt inclusions: evidence from the Siqueiros Transform Fault, East Pacific Rise. *Contributions to Mineralogy and Petrology* **144**, 619–637.

Davidson, J. P., Morgan, D. J., Charlier, B. L. A., Harlou, R. & Hora, J. M. (2007). Microsampling and isotopic analysis of igneous rocks: Implications for the study of magmatic systems. *Annual Review of Earth and Planetary Sciences* **35**, 273–311.

Day, J. M. D., Pearson, D. G., Macpherson, C. G., Lowry, D. & Carracedo, J. C. (2009). Pyroxenite-rich mantle formed by recycled oceanic lithosphere: Oxygen–osmium isotope evidence from Canary Island lavas. *Geology* **37**, 555–558.

Day, J. M. D., Pearson, D. G., Macpherson, C. G., Lowry, D. & Carracedo, J. C. (2010). Evidence for distinct proportions of subducted oceanic crust and lithosphere in HIMU-type mantle beneath El Hierro and La Palma, Canary Islands. *Geochimica et Cosmochimica Acta* **74**, 6565–6589.

Dimanov, A. & Sautter, V. (2000). 'Average' interdiffusion of (Fe,Mn)–Mg in natural diopside. *European Journal of Mineralogy* **12**, 749–760.

Dimanov, A. & Wiedenbeck, M. (2006). (Fe, Mn)–Mg interdiffusion in natural diopside: effect of pO_2. *European Journal of Mineralogy* **18**, 705–718.

Dixon, J. E., Stolper, E. M. & Holloway, J. R. (1995). An experimental study of water and carbon dioxide solubilities in mid-ocean ridge basaltic liquids. Part I: Calibration and solubility models. *Journal of Petrology* **36**, 1607–1631.

Du, Z. & Foulger, G. R. (2004). Surface wave waveform inversion for variation in upper mantle structure beneath Iceland. *Geophysical Journal International* **157**, 305–314.

Eiler, J., Stolper, E. M. & McCanta, M. C. (2011). Intra- and intercrystalline oxygen isotope variations in minerals from basalts and peridotites. *Journal of Petrology* **52**, 1393–1413.

Eiler, J. M. (2001). Oxygen isotope variations of basaltic lavas and upper mantle rocks. In: Valley, J. W. & Cole, D. (eds) *Stable Isotope Geochemistry. Mineralogical Society of America and Geochemical Society, Reviews in Mineralogy and Geochemistry* **43**, 319–364.

Eiler, J. M., Farley, K. A., Valley, J. W., Hofmann, A. W. & Stolper, E. M. (1996). Oxygen isotope constraints on the sources of Hawaiian volcanism. *Earth and Planetary Science Letters* **144**, 453–467.

Eiler, J. M., Farley, K. A., Valley, J. W., Hauri, E., Craig, H., Hart, S. R. & Stolper, E. M. (1997). Oxygen isotope variations in ocean island basalt phenocrysts. *Geochimica et Cosmochimica Acta* **61**, 2281–2293.

Eiler, J. M., Grönvold, K. & Kitchen, N. (2000*a*). Oxygen isotope evidence for the origin of chemical variations in lavas from Theistareykir volcano in Iceland's northern volcanic zone. *Earth and Planetary Science Letters* **184**, 269–286.

Eiler, J. M., Schiano, P., Kitchen, N. & Stolper, E. M. (2000*b*). Oxygen isotope evidence for recycled crust in the sources of mid-ocean-ridge basalts. *Nature* **403**, 530–534.

Elliott, T. R., Hawkesworth, C. J. & Grönvold, K. (1991). Dynamic melting of the Iceland plume. *Nature* **351**, 201–206.

Elphick, S. C., Graham, C. M. & Dennis, P. F. (1988). An ion microprobe study of anhydrous oxygen diffusion in anorthite: a comparison with hydrothermal data and some geological implications. *Contributions to Mineralogy and Petrology* **100**, 490–495.

Elthon, D. & Casey, J. F. (1985). The very depleted nature of certain primary mid-ocean ridge basalts. *Geochimica et Cosmochimica Acta* **49**, 289–298.

Farver, J. R. (2010). Oxygen and hydrogen diffusion in minerals. In: Zhang, Y. & Cherniak, D. J. (eds) *Diffusion in Minerals and Melts. Mineralogical Society of America and Geochemical Society, Reviews in Mineralogy and Geochemistry* **72**, 447–508.

Farver, J. R. & Yund, R. A. (1990). The effect of hydrogen, oxygen, and water fugacity on oxygen diffusion in alkali feldspar. *Geochimica et Cosmochimica Acta* **54**, 2953–2964.

Ford, C. E., Russell, D. G., Craven, J. A. & Fisk, M. R. (1983). Olivine–liquid equilibria: temperature, pressure and composition dependence of the crystal/liquid cation partition coefficients for Mg, Fe^{2+}, Ca and Mn. *Journal of Petrology* **24**, 256–265.

Furnes, H., de Wit, M., Staudigel, H., Rosing, M. & Muehlenbachs, K. (2007). A vestige of Earth's oldest ophiolite. *Science* **315**, 1704–1707.

Garcia, M. O., Eiler, J. M., Pietruszka, A. J. & Lynn, K. (2013). Oxygen isotopes for lavas from Kilauea's ongoing, 30-year old Puu Oo Eruption: Evidence for the nature of the mantle source and crustal contamination. *American Geophysical Union Fall Meeting Abstracts* V12D–07.

Garlick, G. D., MacGregor, I. D. & Vogel, D. E. (1971). Oxygen isotope ratios in eclogites from kimberlites. *Science* **172**, 1025–1027.

Gautason, B. & Muehlenbachs, K. (1998). Oxygen isotopic fluxes associated with high-temperature processes in the rift zones of Iceland. *Chemical Geology* **145**, 275–286.

Gee, M. A. M., Thirlwall, M. F., Taylor, R. N., Lowry, D. & Murton, B. J. (1998). Crustal processes: major controls on Reykjanes Peninsula lava chemistry, SW Iceland. *Journal of Petrology* **39**, 819–839.

Genske, F. S., Beier, C., Haase, K. M., Turner, S. P., Krumm, S. & Brandl, P. A. (2013). Oxygen isotopes in the Azores islands: Crustal assimilation recorded in olivine. *Geology* **41**, 491–494.

Ghiorso, M. S. & Sack, R. O. (1995). Chemical mass transfer in magmatic systems: IV. A revised and internally consistent thermodynamic model for the interpolation and extrapolation of liquid–solid equilibria in magmatic systems at elevated temperatures and pressures. *Contributions to Mineralogy and Petrology* **119**, 197–212.

Ghiorso, M. S., Hirschmann, M. M., Reiners, P. W. & Kress, V. C., III (2002). The pMELTS: a revision of MELTS for improved calculation of phase relations and major element partitioning related to partial melting of the mantle to 3 GPa. *Geochemistry, Geophysics, Geosystems* **3**, 1030, doi:10.1029/2001GC000217.

Giletti, B. J. & Casserly, J. E. D. (1994). Strontium diffusion kinetics in plagioclase feldspars. *Geochimica et Cosmochimica Acta* **58**, 3785–3793.

Gréau, Y., Huang, J.-X., Griffin, W. L., Renac, C., Alard, O. & O'Reilly, S. Y. (2011). Type I eclogites from Roberts Victor kimberlites: products of extensive mantle metasomatism. *Geochimica et Cosmochimica Acta* **75**, 6927–6954.

Gurenko, A. A. & Chaussidon, M. (2002). Oxygen isotope variations in primitive tholeiites of Iceland: evidence from a SIMS study of glass inclusions, olivine phenocrysts and pillow rim glasses. *Earth and Planetary Science Letters* **205**, 63–79.

Gurenko, A. A., Bindeman, I. N. & Chaussidon, M. (2011). Oxygen isotope heterogeneity of the mantle beneath the Canary Islands: insights from olivine phenocrysts. *Contributions to Mineralogy and Petrology* **162**, 349–363.

Halldorsson, S. A., Oskarsson, N., Gronvold, K., Sigurdsson, G., Sverrisdottir, G. & Steinthorsson, S. (2008). Isotopic-heterogeneity of the Thjorsa lava - Implications for mantle sources and crustal processes within the Eastern Rift Zone, Iceland. *Chemical Geology* **255**, 305–316.

Harmon, R. S. & Hoefs, J. (1995). Oxygen isotope heterogeneity of the mantle deduced from global ^{18}O systematics of basalts from different geotectonic settings. *Contributions to Mineralogy and Petrology* **120**, 95–114.

Hattori, K. & Muehlenbachs, K. (1982). Oxygen isotope ratios of the Icelandic crust. *Journal of Geophysical Research B: Solid Earth* **87**, 6559–6565.

Hauri, E. H., Wagner, T. P. & Grove, T. L. (1994). Experimental and natural partitioning of Th, U, Pb and other trace elements between garnet, clinopyroxene and basaltic melts. *Chemical Geology* **117**, 149–166.

Heinrich, C. A., Pettke, T., Halter, W. E., Aigner-Torres, M., Audétat, A., Günther, D., Hattendorf, B., Bleiner, D., Guillong, M. & Horn, I. (2003). Quantitative multi-element analysis of minerals, fluid and melt inclusions by laser-ablation inductively-coupled-plasma mass-spectrometry. *Geochimica et Cosmochimica Acta* **67**, 3473–3497.

Hémond, C., Condomines, M., Fourcade, S., Allègre, C. J., Oskarsson, N. & Javoy, M. (1988). Thorium, strontium and oxygen isotopic geochemistry in recent tholeiites from Iceland: crustal influence on mantle-derived magmas. *Earth and Planetary Science Letters* **87**, 273–285.

Hémond, C., Arndt, N. T., Lichtenstein, U., Hofmann, A. W., Oskarsson, N. & Steinthorsson, S. (1993). The heterogeneous Iceland plume: Nd–Sr–O isotopes and trace element constraints. *Journal of Geophysical Research B: Solid Earth* **98**, 15833–15850.

Hinton, R. W. (1990). Ion microprobe trace-element analysis of silicates: Measurement of multi-element glasses. *Chemical Geology* **83**, 11–25.

Hirschmann, M. M. & Stolper, E. M. (1996). A possible role for garnet pyroxenite in the origin of the 'garnet signature' in MORB. *Contributions to Mineralogy and Petrology* **124**, 185–208.

Hoffman, S. E., Wilson, M. & Stakes, D. S. (1986). Inferred oxygen isotope profile of Archaean oceanic crust, Onverwacht Group, South Africa. *Nature* **321**, 55–58.

Hofmann, A. W. & White, W. M. (1982). Mantle plumes from ancient oceanic crust. *Earth and Planetary Science Letters* **57**, 421–436.

Holmden, C. & Muehlenbachs, K. (1993). The $^{18}O/^{16}O$ ratio of 2-billion-year old seawater inferred from ancient oceanic crust. *Science* **259**, 1733–1736.

Irving, A. J. & Frey, F. A. (1984). Trace element abundances in megacrysts and their host basalts: Constraints on partition coefficients and megacryst genesis. *Geochimica et Cosmochimica Acta* **48**, 1201–1221.

Jacob, D. E. (2004). Nature and origin of eclogite xenoliths from kimberlites. *Lithos* **77**, 295–316.

Jacob, D. E., Bizimis, M. & Salters, V. J. M. (2005). Lu–Hf and geochemical systematics of recycled ancient oceanic crust: evidence from Roberts Victor eclogites. *Contributions to Mineralogy and Petrology* **148**, 707–720.

Jaffrés, J. B. D., Shields, G. A. & Wallmann, K. (2007). The oxygen isotope evolution of seawater: A critical review of a long-standing controversy and an improved geological water cycle model for the past 3·4 billion years. *Earth-Science Reviews* **83**, 83–122.

Joachimski, M. M., Breisig, S., Buggisch, W., Talent, J. A., Mawson, R., Gereke, M., Morrow, J. R., Day, J. & Weddige, K. (2009). Devonian climate and reef evolution: Insights from oxygen isotopes in apatite. *Earth and Planetary Science Letters* **284**, 599–609.

Jochum, K. P. & Nehring, F. (2006). BCR-2G, BIR-1G, BHVO-2G: GeoReM preferred values (11/2006). GeoReM database (http://georem.mpch-mainz.gwdg.de).

Jochum, K. P. & Stoll, B. (2008). Reference materials for elemental and isotopic analyses by LA-(MC)-ICP-MS: Successes and outstanding needs. In: Sylvester, P. (ed.) *Laser Ablation ICP-MS in the Earth Sciences: Current Practices and Outstanding Issues. Mineralogical Association of Canada, Short Course* **40**, 147–168.

Jochum, K. P., Willbold, M., Raczek, I., Stoll, B. & Herwig, K. (2005). Chemical characterisation of the USGS reference glasses GSA-1G, GSC-1G, GSD-1G, GSE-1G, BCR-2G, BHVO-2G and BIR-1G using EPMA, ID-TIMS, ID-ICPMS and LA-ICPMS. *Geostandards and Geoanalytical Research* **29**, 285–302.

Jónasson, K. (1994). Rhyolite volcanism in the Krafla central volcano, northeast Iceland. *Bulletin of Volcanology* **56**, 516–528.

Jónasson, K. (2005). Magmatic evolution of the Heiðarsporður ridge, NE Iceland. *Journal of Volcanology and Geothermal Research* **147**, 109–124.

Kita, N. T., Ushikubo, T., Fu, B. & Valley, J. W. (2009). High precision SIMS oxygen isotope analysis and the effect of sample topography. *Chemical Geology* **264**, 43–57.

Kogiso, T., Hirose, K. & Takahashi, E. (1998). Melting experiments on homogeneous mixtures of peridotite and basalt: application to the genesis of ocean island basalts. *Earth and Planetary Science Letters* **162**, 45–61.

Kogiso, T., Hirschmann, M. M. & Reiners, P. W. (2004). Length scales of mantle heterogeneities and their relationship to ocean island basalt geochemistry. *Geochimica et Cosmochimica Acta* **68**, 345–360.

Kokfelt, T. F., Hoernle, K., Hauff, F., Fiebig, J., Werner, R. & Garbe-Schönberg, D. (2006). Combined trace element and Pb–Nd–Sr–O isotope evidence for recycled oceanic crust (upper and lower) in the Iceland mantle plume. *Journal of Petrology* **47**, 1705–1749.

Koornneef, J. M., Stracke, A., Bourdon, B. & Grönvold, K. (2012). The influence of source heterogeneity on the U–Th–Pa–Ra disequilibria in post-glacial tholeiites from Iceland. *Geochimica et Cosmochimica Acta* **87**, 243–266.

Kristmannsdóttir, H. & Ármannsson, H. (2004). Groundwater in the Lake Myvatn area, northern Iceland: Chemistry, origin and interaction. *Aquatic Ecology* **38**, 115–128.

Lécuyer, C. & Fourcade, S. (1991). Oxygen isotope evidence for multi-stage hydrothermal alteration at a fossil slow-spreading center: The Silurian Trinity ophiolite (California, USA). *Chemical Geology: Isotope Geoscience Section* **87**, 231–246.

Lundstrom, C., Boudreau, A. & Pertermann, M. (2005). Diffusion-reaction in a thermal gradient: Implications for the genesis of anorthitic plagioclase, high alumina basalt and igneous mineral layering. *Earth and Planetary Science Letters* **237**, 829–854.

Lundstrom, C. C. & Tepley, F. J., III (2006). Investigating the origin of anorthitic plagioclase through a combination of experiments and natural observations. *Journal of Volcanology and Geothermal Research* **157**, 202–221.

Macdonald, R., Sparks, R. S. J., Sugurdsson, H., Mattey, D. P., McGarvie, D. W. & Smith, R. L. (1987). The 1875 eruption of the Askja volcano, Iceland: combined fractional crystallization and selective contamination in the generation of rhyolitic magma. *Mineralogical Magazine* **51**, 183–202.

MacGregor, I. D. & Manton, W. I. (1986). Roberts Victor eclogites: ancient oceanic crust. *Journal of Geophysical Research B: Solid Earth* **91**, 14063–14079.

Maclennan, J. (2008*a*). Concurrent mixing and cooling of melts under Iceland. *Journal of Petrology* **49**, 1931–1953.

Maclennan, J. (2008*b*). Lead isotope variability in olivine-hosted melt inclusions from Iceland. *Geochimica et Cosmochimica Acta* **72**, 4159–4176.

Maclennan, J., McKenzie, D. & Grönvold, K. (2001*a*). Plume-driven upwelling under central Iceland. *Earth and Planetary Science Letters* **194**, 67–82.

Maclennan, J., McKenzie, D., Grönvold, K. & Slater, L. (2001*b*). Crustal accretion under northern Iceland. *Earth and Planetary Science Letters* **191**, 295–310.

Maclennan, J., Jull, M., McKenzie, D., Slater, L. & Grönvold, K. (2002). The link between volcanism and deglaciation in Iceland. *Geochemistry, Geophysics, Geosystems* **3**, 1062, doi:10.1029/2001GC000282.

Maclennan, J., McKenzie, D., Grönvold, K., Shimizu, N., Eiler, J. M. & Kitchen, N. (2003*a*). Melt mixing and crystallization under Theistareykir, northeast Iceland. *Geochemistry, Geophysics, Geosystems* **4**, 8624, doi:10.1029/2003GC000558.

Maclennan, J., McKenzie, D., Hilton, F., Grönvold, K. & Shimizu, N. (2003*b*). Geochemical variability in a single flow from northern Iceland. *Journal of Geophysical Research B: Solid Earth* **108**, doi:10.1029/2000JB000142.

Macpherson, C. G. & Mattey, D. P. (1998). Oxygen isotope variations in Lau Basin lavas. *Chemical Geology* **144**, 177–194.

Macpherson, C. G., Hilton, D. R., Day, J. M. D., Lowry, D. & Gronvold, K. (2005). High-$^{3}He/^{4}He$, depleted mantle and low-$\delta^{18}O$, recycled oceanic lithosphere in the source of central Iceland magmatism. *Earth and Planetary Science Letters* **233**, 411–427.

Martin, E. & Sigmarsson, O. (2007). Crustal thermal state and origin of silicic magma in Iceland: the case of Torfajökull, Ljósufjöll and Snæfellsjökull volcanoes. *Contributions to Mineralogy and Petrology* **153**, 593–605.

Mattey, D., Lowry, D. & Macpherson, C. (1994). Oxygen isotope composition of mantle peridotite. *Earth and Planetary Science Letters* **128**, 231–241.

McDonough, W. F. & Sun, S. S. (1995). The composition of the Earth. *Chemical Geology* **120**, 223–253.

McKenzie, D. & O'Nions, R. K. (1991). Partial melt distributions from inversion of rare earth element concentrations. *Journal of Petrology* **32**, 1021–1091.

McKenzie, D., Stracke, A., Blichert-Toft, J., Albarède, F., Grönvold, K. & O'Nions, R. K. (2004). Source enrichment

processes responsible for isotopic anomalies in oceanic island basalts. *Geochimica et Cosmochimica Acta* **68**, 2699–2724.

Miller, J. A., Cartwright, I., Buick, I. S. & Barnicoat, A. C. (2001). An O-isotope profile through the HP–LT Corsican ophiolite, France and its implications for fluid flow during subduction. *Chemical Geology* **178**, 43–69.

Muehlenbachs, K., Anderson, A. T. & Sigvaldason, G. E. (1974). Low-$\delta^{18}O$ basalts from Iceland. *Geochimica et Cosmochimica Acta* **38**, 577–588.

Muehlenbachs, K., Furnes, H., Fonneland, H. C. & Hellevang, B. (2003). Ophiolites as faithful records of the oxygen isotope ratio of ancient seawater: the Solund–Stavfjord Ophiolite Complex as a Late Ordovician example. In: Dilek, Y. & Robinson, P. T. (eds) *Ophiolites in Earth History. Geological Society of London, Special Publication* **218**, 401–414.

Nichols, A. R. L. & Wysoczanski, R. J. (2007). Using micro-FTIR spectroscopy to measure volatile contents in small and unexposed inclusions hosted in olivine crystals. *Chemical Geology* **242**, 371–384.

Nicholson, H. & Latin, D. (1992). Olivine tholeiites from Krafla, Iceland: Evidence for variations in melt fraction within a plume. *Journal of Petrology* **33**, 1105–1124.

Nicholson, H., Condomines, M., Fitton, J. G., Fallick, A. E., Grönvold, K. & Rogers, G. (1991). Geochemical and isotopic evidence for crustal assimilation beneath Krafla, Iceland. *Journal of Petrology* **32**, 1005–1020.

Nielsen, R. L., Gallahan, W. E. & Newberger, F. (1992). Experimentally determined mineral–melt partition coefficients for Sc, Y and REE for olivine, orthopyroxene, pigeonite, magnetite and ilmenite. *Contributions to Mineralogy and Petrology* **110**, 488–499.

Ongley, J. S., Basu, A. R. & Kurtis Kyser, T. (1987). Oxygen isotopes in coexisting garnets, clinopyroxenes and phlogopites of Roberts Victor eclogites: implications for petrogenesis and mantle metasomatism. *Earth and Planetary Science Letters* **83**, 80–84.

Panjasawatwong, Y., Danyushevsky, L. V., Crawford, A. J. & Harris, K. L. (1995). An experimental study of the effects of melt composition on plagioclase–melt equilibria at 5 and 10 kbar: implications for the origin of magmatic high-An plagioclase. *Contributions to Mineralogy and Petrology* **118**, 420–432.

Peate, D. W., Baker, J. A., Jakobsson, S. P., Waight, T. E., Kent, A. J. R., Grassineau, N. V. & Skovgaard, A. C. (2009). Historic magmatism on the Reykjanes Peninsula, Iceland: a snap-shot of melt generation at a ridge segment. *Contributions to Mineralogy and Petrology* **157**, 359–382.

Peate, D. W., Breddam, K., Baker, J. A., Kurz, M. D., Barker, A. K., Prestvik, T., Grassineau, N. & Skovgaard, A. C. (2010). Compositional characteristics and spatial distribution of enriched Icelandic mantle components. *Journal of Petrology* **51**, 1447–1475.

Pettke, T. (2006). *In situ* laser-ablation ICPMS analysis of melt inclusions and prospects for constraining subduction zone magmatism. In: Webster, J. D. (ed.) *Melt Inclusions in Plutonic Rocks. Mineralogical Association of Canada, Short Course* **36**, 51–80.

Putirka, K. D. (2005). Igneous thermometers and barometers based on plagioclase + liquid equilibria: Tests of some existing models and new calibrations. *American Mineralogist* **90**, 336–346.

Putirka, K. D. (2008). Thermometers and barometers for volcanic systems. In: Putirka, K. D. & Tepley, F. J., III (eds) *Minerals, Inclusions and Volcanic Processes. Mineralogical Society of America and Geochemical Society, Reviews in Mineralogy and Geochemistry* **69**, 61–120.

Ryerson, F. J. & McKeegan, D. K. (1994). Determination of oxygen self-diffusion in åkermanite, anorthite, diopside, and spinel: Implications for oxygen isotopic anomalies and the thermal histories of Ca–Al-rich inclusions. *Geochimica et Cosmochimica Acta* **58**, 3713–3734.

Saal, A. E., Hauri, E. H., Langmuir, C. H. & Perfit, M. R. (2002). Vapour undersaturation in primitive mid-ocean-ridge basalt and the volatile content of Earth's upper mantle. *Nature* **419**, 451–455.

Saunders, A. D., Norry, M. J. & Tarney, J. (1988). Origin of MORB and chemically-depleted mantle reservoirs: trace element constraints. *Journal of Petrology, Special Lithosphere Issue* 415–445.

Schulze, D. J., Valley, J. W. & Spicuzza, M. J. (2000). Coesite eclogites from the Roberts Victor kimberlite, South Africa. *Lithos* **54**, 23–32.

Shimizu, N. & Hart, S. R. (1982). Applications of the ion microprobe to geochemistry and cosmochemistry. *Annual Review of Earth and Planetary Sciences* **10**, 483–526.

Shirey, S. B., Carlson, R. W., Richardson, S. H., Menzies, A., Gurney, J. J., Pearson, D. G., Harris, J. W. & Wiechert, U. (2001). Archean emplacement of eclogitic components into the lithospheric mantle during formation of the Kaapvaal Craton. *Geophysical Research Letters* **28**, 2509–2512.

Shorttle, O. & Maclennan, J. (2011). Compositional trends of Icelandic basalts: Implications for short-length scale lithological heterogeneity in mantle plumes. *Geochemistry, Geophysics, Geosystems* **12**, Q11008, doi:10.1029/2011GC003748.

Shorttle, O., Maclennan, J. & Jones, S. M. (2010). Control of the symmetry of plume–ridge interaction by spreading ridge geometry. *Geochemistry, Geophysics, Geosystems* 11Q0AC05, doi:10.1029/2009GC002986.

Sigmarsson, O., Hémond, C., Condomines, M., Fourcade, S. & Oskarsson, N. (1991). Origin of silicic magma in Iceland revealed by Th isotopes. *Geology* **19**, 621–624.

Sigmarsson, O., Condomines, M. & Fourcade, S. (1992*a*). A detailed Th, Sr and O isotope study of Hekla: differentiation processes in an Icelandic volcano. *Contributions to Mineralogy and Petrology* **112**, 20–34.

Sigmarsson, O., Condomines, M. & Fourcade, S. (1992*b*). Mantle and crustal contribution in the genesis of Recent basalts from off-rift zones in Iceland: Constraints from Th, Sr and O isotopes. *Earth and Planetary Science Letters* **110**, 149–162.

Sigurdsson, I. A., Steinthorsson, S. & Grönvold, K. (2000). Calcium-rich melt inclusions in Cr-spinels from Borgarhraun, northern Iceland. *Earth and Planetary Science Letters* **183**, 15–26.

Sims, K. W. W., Maclennan, J., Blichert-Toft, J., Mervine, E. M., Blusztajn, J. & Grönvold, K. (2013). Short length scale mantle heterogeneity beneath Iceland probed by glacial modulation of melting. *Earth and Planetary Science Letters* **379**, 146–157.

Sinton, J., Grönvold, K. & Sæmundsson, K. (2005). Postglacial eruptive history of the Western Volcanic Zone, Iceland. *Geochemistry, Geophysics, Geosystems* **6**, Q12009, doi:10.1029/2005GC001021.

Skovgaard, A. C., Storey, M., Baker, J., Blusztajn, J. & Hart, S. R. (2001). Osmium–oxygen isotopic evidence for a recycled and strongly depleted component in the Iceland mantle plume. *Earth and Planetary Science Letters* **194**, 259–275.

Slater, L. (1996). Melt generation beneath Iceland. PhD thesis, University of Cambridge.

Slater, L., McKenzie, D., Grönvold, K. & Shimizu, N. (2001). Melt generation and movement beneath Theistareykir, NE Iceland. *Journal of Petrology* **42**, 321–354.

Smith, P. M. & Asimow, P. D. (2005). Adiabat_1ph: A new public frontend to the MELTS, pMELTS, and pHMELTS models. *Geochemistry, Geophysics, Geosystems* **6**, Q02004, doi:10.1029/2004GC000816.

Sneeringer, M., Hart, S. R. & Shimizu, N. (1984). Strontium and samarium diffusion in diopside. *Geochimica et Cosmochimica Acta* **48**, 1589–1608.

Sobolev, A. V., Hofmann, A. W., Kuzmin, D. V., Yaxley, G. M., Arndt, N. T., Chung, S.-L., Danyushevsky, L. V., Elliott, T., Frey, F. A., Garcia, M. O., Gurenko, A. A., Kamenetsky, V. S., Kerr, A. C., Krivolutskaya, N. A., Matvienkov, V. V.,

Nikogosian, I. K., Rocholl, A., Sigurdsson, I. A., Sushchevskaya, N. M. & Teklay, M. (2007). The amount of recycled crust in sources of mantle-derived melts. *Science* **316**, 412–417.

Sobolev, A. V., Hofmann, A. W., Brügmann, G., Batanova, V. G. & Kuzmin, D. V. (2008). A quantitative link between recycling and osmium isotopes. *Science* **321**, 536.

Stakes, D. S. & Taylor, H. P., Jr (1992). The northern Samail ophiolite: an oxygen isotope, microprobe, and field study. *Journal of Geophysical Research B: Solid Earth* **97**, 7043–7080.

Stracke, A., Zindler, A., Salters, V. J. M., McKenzie, D., Blichert-Toft, J., Albarède, F. & Grönvold, K. (2003*a*). Theistareykir revisited. *Geochemistry, Geophysics, Geosystems* **4**, 8507, doi:10.1029/2001GC000201.

Stracke, A., Zindler, A., Salters, V. J. M., McKenzie, D. & Grönvold, K. (2003*b*). The dynamics of melting beneath Theistareykir, northern Iceland. *Geochemistry, Geophysics, Geosystems* **4**, 8513, doi:10.1029/2002GC000347.

Sylvester, P. J. (2008). Matrix effects in laser ablation-ICP-MS. In: Sylvester, P. (ed.) *Laser Ablation ICP-MS in the Earth Sciences: Current Practices and Outstanding Issues. Mineralogical Association of Canada, Short Course* **40**, 67–78.

Thirlwall, M. F., Gee, M. A. M., Taylor, R. N. & Murton, B. J. (2004). Mantle components in Iceland and adjacent ridges investigated using double-spike Pb isotope ratios. *Geochimica et Cosmochimica Acta* **68**, 361–386.

Thirlwall, M. F., Gee, M. A. M., Lowry, D., Mattey, D. P., Murton, B. J. & Taylor, R. N. (2006). Low $\delta^{18}O$ in the Icelandic mantle and its origins: Evidence from Reykjanes Ridge and Icelandic lavas. *Geochimica et Cosmochimica Acta* **70**, 993–1019.

Thomson, A. & Maclennan, J. (2013). The distribution of olivine compositions in Icelandic basalts and picrites. *Journal of Petrology* **54**, 745–768.

Turner, S., Tonarini, S., Bindeman, I., Leeman, W. P. & Schaefer, B. F. (2007). Boron and oxygen isotope evidence for recycling of subducted components over the past 2·5 Gyr. *Nature* **447**, 702–705.

Valley, J. W. (1986). Stable isotope geochemistry of metamorphic rocks. In: Valley, J. W., Taylor, H. P., Jr & O'Neil, J. R. (eds) *Stable Isotopes in High Temperature Geological Processes. Mineralogical Society of America, Reviews in Mineralogy* **16**, 445–489.

Van Orman, J. A., Grove, T. L. & Shimizu, N. (2001). Rare earth element diffusion in diopside: influence of temperature, pressure, and ionic radius, and an elastic model for diffusion in silicates. *Contributions to Mineralogy and Petrology* **141**, 687–703.

Veizer, J., Ala, D., Azmy, K., Bruckschen, P., Buhl, D., Bruhn, F., Carden, G. A. F., Diener, A., Ebneth, S., Godderis, Y., Jasper, T., Korte, C., Pawellek, F., Podlaha, O. G. & Strauss, H. (1999). $^{87}Sr/^{86}Sr$, $\delta^{13}C$ and $\delta^{18}O$ evolution of Phanerozoic seawater. *Chemical Geology* **161**, 59–88.

Wang, Z. & Eiler, J. M. (2008). Insights into the origin of low-$\delta^{18}O$ basaltic magmas in Hawaii revealed from *in situ* measurements of oxygen isotope compositions of olivines. *Earth and Planetary Science Letters* **269**, 377–387.

Watson, E. B. (1996). Surface enrichment and trace-element uptake during crystal growth. *Geochimica et Cosmochimica Acta* **60**, 5013–5020.

Weaver, B. L. (1991). The origin of ocean island basalt end-member compositions: trace element and isotopic constraints. *Earth and Planetary Science Letters* **104**, 381–397.

Winpenny, B. & Maclennan, J. (2011). A partial record of mixing of mantle melts preserved in Icelandic phenocrysts. *Journal of Petrology* **52**, 1791–1812.

Wood, B. J. & Blundy, J. D. (1997). A predictive model for rare earth element partitioning between clinopyroxene and anhydrous silicate melt. *Contributions to Mineralogy and Petrology* **129**, 166–181.

Workman, R. K. & Hart, S. R. (2005). Major and trace element composition of the depleted MORB mantle (DMM). *Earth and Planetary Science Letters* **231**, 53–72.

Yoder, H. S. (1965). Diopside–anorthite–water at five and ten kilobars and its bearing on explosive volcanism. *Carnegie Institution of Washington Yearbook* **64**, 82–89.